RESEARCH   **Open Access**

CrossMark

Oligomeric amyloid-beta induces MAPK-mediated activation of brain cytosolic and calcium-independent phospholipase A$_2$ in a spatial-specific manner

Juan Pablo Palavicini[1], Chunyan Wang[1], Linyuan Chen[1], Kristen Hosang[1], Jianing Wang[1], Takami Tomiyama[2], Hiroshi Mori[3] and Xianlin Han[1*]

Abstract

Alzheimer's disease (AD) is histopathologically characterized by the build-up of fibrillar amyloid beta (Aβ) in the form of amyloid plaques and the development of intraneuronal neurofibrillary tangles consisting of aggregated hyperphosphorylated Tau. Although amyloid fibrils were originally considered responsible for AD pathogenesis, recent convincing evidence strongly implicates soluble oligomeric Aβ as the primary neurotoxic species driving disease progression. A third largely ignored pathological hallmark, originally described by Alois Alzheimer, is the presence of "adipose inclusions", suggestive of aberrant lipid metabolism. The molecular mechanisms underlying these "lipoid granules", as well as their potential link to soluble and/or fibrillar Aβ remain largely unknown. Seeking to better-understand these conundrums, we took advantage of the powerful technology of multidimensional mass spectrometry-based shotgun lipidomics and an AD transgenic mouse model overexpressing mutant amyloid precursor protein (APP E693Δ-Osaka-), where AD-like pathology and neurodegeneration occur as a consequence of oligomeric Aβ accumulation in the absence of amyloid plaques. Our results revealed for the first time that APP overexpression and oligomeric Aβ accumulation lead to an additive global accumulation of nonesterified polyunsaturated fatty acids (PUFAs) independently of amyloid plaques. Furthermore, we revealed that this accumulation is mediated by an increase in phospholipase A$_2$ (PLA$_2$) activity, evidenced by an accumulation of *sn*-1 lysophosphatidylcholine and by MAPK-mediated phosphorylation/activation of group IV Ca^{2+}-dependent cytosolic (cPLA$_2$) and the group VI Ca^{2+}-independent PLA$_2$ (iPLA$_2$) independently of PKC. We further revealed that Aβ-induced oxidative stress also disrupts lipid metabolism via reactive oxygen species-mediated phospholipid cleavage leading to increased *sn*-2 lysophosphatidylcholine as well as lipid peroxidation and the subsequent accumulation of 4-hydroxynonenal. Brain histological studies implicated cPLA$_2$ activity with arachidonic acid accumulation within myelin-rich regions, and iPLA$_2$ activity with docosahexaenoic acid accumulation within pyramidal neuron-rich regions. Taken together, our results suggest that PLA$_2$-mediated accumulation of free PUFAs drives AD-related disruption of brain lipid metabolism.

Keywords: Alzheimer's disease, Amyloid-beta, Fatty acid, Lysophospholipid, Phospholipase A$_2$, Oxidative stress

---

* Correspondence: xhan@sbpdiscovery.org
[1]Center for Metabolic Origins of Disease, Sanford Burnham Prebys Medical Discovery Institute, 6400 Sanger Road, Orlando, FL 32827, USA
Full list of author information is available at the end of the article

BioMed Central

Palavicini *et al. Acta Neuropathologica Communications* (2017) 5:56

Page 2 of 17

Introduction

Decades of Alzheimer's disease (AD) research have been grounded on the so called "amyloid cascade hypothesis", which originally placed amyloid precursor protein (APP) mismetabolism and subsequent Aβ aggregation (i.e., fibrillation) as the initial trigger responsible for instigating further pathological events (i.e., tauopathy, synaptic damage, and neuronal death) [49, 52, 97]. However, amyloid deposits were later shown to correlate poorly with cognitive decline and to be disconnected from Aβ-induced toxicity [29, 68, 72, 85]. On the other hand, characterization of soluble Aβ structures led to the discovery of Aβ derived diffusible ligands (ADDLs) or oligomeric Aβ [63]: extremely neurotoxic species that strongly correlate with synaptic impairment and parallel cognitive decline in animal models and humans [11, 36, 53, 62, 63, 68, 120, 122, 123]. Importantly, it has been shown that oligomeric Aβ species are both necessary and sufficient to disrupt cognitive function in vivo [21, 64, 107]. These findings led to a "revised" amyloid cascade hypothesis where diffusible oligomeric Aβ replaced fibrillar Aβ as the central neurotoxic event driving AD pathogenesis [48, 98].

The E693Δ (Osaka) mutation in APP, which was found in Japanese pedigrees, causes familial AD by enhancing Aβ oligomerization in the absence of deposits of amyloid plaques [116]. The mutant Aβ peptide, which lacks glutamate-22 (E22Δ), forms abundant oligomers in vitro and causes endoplasmic reticulum stress-induced apoptosis in cultured cells [83]. When injected into rat cerebral ventricle, synthetic mutant Aβ E22Δ peptide inhibits hippocampal long-term potentiation more potently than wild-type (WT) peptide [116]. Exogenously applied Aβ E22Δ peptide induces dose-dependent loss of synapses in mouse hippocampal slices [112]. In addition, $APP_{E693Δ}$ transgenic mice (APP_{OSK}) showed intraneuronal accumulation of Aβ oligomers, synapse loss, memory impairment, and significant neuronal loss at 24 months of age [115]. Thus, APP_{OSK} mice successfully recapitulate Aβ neurotoxicity in the absence of amyloid plaques.

When Alois Alzheimer first described the disease over 100 years ago, he identified abnormal protein deposits as well as adipose saccules (lipid inclusions) in the brains of his patients [4]. These observations suggested a possible relation between AD and lipid imbalance, which was established decades later when the strongest genetic risk factor in AD was linked to apolipoprotein E (apoE), the major lipid transporter in the CNS. Dysregulation of multiple lipid families has been linked to AD, including alterations in the levels of sulfatide, plasmalogen ethanolamine glycerophospholipid, cholesterol, ceramide, and fatty acids (FAs) [15, 18, 19, 23, 26, 41, 43, 44, 46].

FAs and their metabolites are of particular relevance, given that they participate in processes involved in the pathogenesis of AD, including synaptic plasticity, inflammation, cerebrovascular function, and oxidative stress [74, 88, 89, 106]. FAs are released from phospholipids by phospholipase A_2 (PLA_2) [61], a family of enzymes that catalyze the cleavage of FAs from the *sn*-2 position of phospholipids. These enzymes are not only important for maintenance of cellular membrane phospholipids, they also play a key role in regulating the release of signaling molecules like arachidonic acid (AA) and docosahexaenoic acid (DHA), important precursors for lipid-derived modulators of cell signaling and inflammatory processes. Given that phospholipids within CNS membranes are enriched in polyunsaturated fatty acids (PUFAs) [110] and that the *sn*-2 position is mostly constituted with unsaturated FAs, PLA_2 cleavage activity within the brain results in accumulation of lysophospholipids and unsaturated FAs [93, 96, 134].

In the mammalian system, more than 19 different isoforms of PLA_2 have been identified, and different PLA_2s have been shown to participate in physiological events related to cell injury, inflammation, and apoptosis [24, 81]. Research to understand PLA_2s in the CNS has focused on 3 PLA_2 isoforms: the group IV Ca^{2+}-dependent cytosolic PLA_2 ($cPLA_2$), which has been strongly associated with AD (reviewed in [94]) [22, 95, 108, 109, 111, 113]; the group VI Ca^{2+}-independent PLA_2 ($iPLA_2$), which has been proposed to account for >70% of brain PLA_2 activity [132] and is highly enriched in AD-affected brain regions (i.e., cortex and hippocampus) [87]; and the group II secretory PLA_2 ($sPLA_2$), which has also been linked to AD more recently [14, 80].

Importantly, the activity of $cPLA_2$ has been shown to be tightly regulated by multiple mechanisms. First, $cPLA_2$ becomes activated after translocating to the plasma membrane from the cytosol [35]. Although Ca^{2+} is not necessary for $cPLA_2$ catalytic activity, nanomolar Ca^{2+} concentrations are needed for its binding to the membrane [32]. Second, it is well-established that phosphorylation of $cPLA_2\alpha$ at multiple sites (Ser505 and Ser515) stimulates its catalytic activity [30, 34, 50, 60, 66]. In vitro work has revealed that protein kinase C (PKC) plays an important role in mediating $cPLA_2$ phosphorylation and AA release in murine astrocytes through both MAPK-dependent and MAPK-independent pathways [131]. Third, $cPLA_2$ regulation via protease-mediated cleavage has also been documented [1, 5, 6, 30, 40, 119, 128], although this regulation seems to occur only under apoptotic and/or necrotic conditions. Conflicting data have been reported regarding the effects of $cPLA_2$ proteolysis which has been found to both activate [30, 40, 128] and inhibit [1, 5, 6, 119] its activity. Notably, cPLA is highly specific to AA cleavage/release [28, 100, 101] and to PC [81]. In fact, $cPLA_2\alpha$-deficient mice fail to generate AA metabolites after brain injury [9, 61], thus $cPLA_2\alpha$ seems to be the most relevant $cPLA_2$ in the brain.

Palavicini *et al. Acta Neuropathologica Communications* (2017) 5:56

Page 3 of 17

Like $cPLA_2$, the activity of $iPLA_2$ also seems to be tightly controlled. First, it has been well-established that $iPLA_2$ is inhibited by calmodulin and activated by Ca^{2+} release from ER where calcium influx factor (CIF) has been proposed to displace inhibitory calmodulin [104, 129, 130]. Second, it has been proposed that PKC mediates phosphorylation of $iPLA_2$ (directly and/or indirectly) promoting its activity [75]. Third, caspase-3-dependent cleavage and activation of $iPLA_2$ have been documented [136]. Notably, murine studies have reported expression of an 80-kDa $iPLA_2$ isoform ($iPLA_2\beta$ encoded by the *PLA2G6* gene) in brain tissue [132]. $iPLA_2\beta$ has been shown to be physiologically and clinically relevant, as demonstrated by characterization of $iPLA_2\beta$-KO mice which model neurodegeneration with brain iron accumulation [70, 102] and by the fact that mutations in the *PLA2G6* gene lead to two childhood neurologic disorders [39, 56, 78].

Although multiple lipid classes and lipid cleavage enzymes have been associated to AD, whether lipid dysregulation plays a causative or epiphenomal role in the disease remains largely unknown. In the current study, we took advantage of the APP_{OSK} mouse model where AD-like pathology and neurodegeneration occur in the absence of amyloid plaques, and demonstrated that oligomeric amyloid-beta ($A\beta$) induces accumulation of free PUFAs and lysophosphatidylcholine by activation of brain $cPLA_2$ and $iPLA_2$ within myelin-rich and pyramidal neuron-rich regions, respectively, via MAPK-mediated phosphorylation in a PKC-independent manner.

Materials and methods
Mice
Brain tissue from 12 and 24 month old APP_{OSK}-Tg, APP_{WT}-Tg, and non-Tg mice (n = 4/genotype including an equal mix of male and female mice) was kindly obtained from Dr. Takami Tomiyama, Associate Professor from the Osaka City University. As previously described, three lines of APP-Tg lines have been established for APP_{WT} and APP_{OSK} mice with high (L1), low (L2), and intermediate (L3) human expression of the transgene [115]. All the studies were performed using L1 APP-Tg lines. It is important to note that APP_{WT} L1 mice express higher levels of human APP (2-fold) than APP_{OSK} L1 mice do [115].

Lipid extraction
Mouse cerebrum tissue was sub-dissected by removal of olfactory lobe, cerebellum, brain stem, and colliculus from each hemibrain. Frozen cerebrum samples were weighed, lyophilized, pulverized, and homogenized in 500 µl of ice-cold diluted phosphate-buffered saline (0.1X PBS) on a cooling tissue homogenizer (Cryolys Precellys Evolution Homogenizer). Protein assays on individual homogenates were performed using a BCA protein assay kit (Pierce, Rockford, IL, USA). Lipids were extracted by a modified procedure of Bligh and Dyer extraction as described previously [16, 17] in the presence of internal standards which were added based on total protein content of the sample.

Mass spectrometric analysis of lipids
A triple-quadrupole mass spectrometer (Thermo Scientific TSQ Vantage, CA, USA) equipped with a Nanomate device (Advion Bioscience Ltd., NY, USA) and Xcalibur system software was used as previously described [47, 133]. Diluted lipid extracts were directly infused into the ESI source through a Nanomate device [47]. Typically, signals were averaged over a 1-min period in the profile mode for each full scan MS spectrum. For tandem MS, a collision gas pressure was set at 1.0 mTorr, but the collision energy varied with the classes of lipids as described previously [45, 133]. Similarly, a 2- to 5-min period of signal averaging in the profile mode was employed for each tandem MS mass spectrum. All full and tandem MS mass spectra were automatically acquired using a customized sequence subroutine operated under Xcalibur software. Data processing including ion peak selection, baseline correction, data transfer, peak intensity comparison, ^{13}C deisotoping, and quantitation were conducted using a custom programmed Microsoft Excel macro as previously described [133] after considering the principles of lipidomics [125].

Elisa
The levels of $A\beta$ oligomers were quantified by direct ELISA with anti-human amyloid-β E22P (11A1) mouse IgG monoclonal antibody (IBL, Japan) at 1 µg/ml as previously described [13, 118]. Briefly, PBS supernatants (at a concentration of 5000 µg/ml of total protein) were diluted 6-fold in sodium bicarbonate pH 9.6 (0.5X ELISA Plate Coating buffer, Alpha Diagnostic International, TX) and allowed to coat ELISA plates at 50 µl/well. After incubation with HRP-conjugated anti-mouse IgG, 11A1 immunoreactivity was detected using 3,3′,5,5′-Tetramethylbenzidine (TMB-1, Alpha Diagnostic International, TX). Reactions were stopped with diluted sulfuric acid (1X Stop Solution, Alpha Diagnostic International, TX).

Western blot analysis
Pulverized cerebrum tissues were homogenized in 1X NP40 on a cooling tissue homogenizer (Cryolys Precellys Evolution Homogenizer). NP40 homogenates were centrifuged at 12,300 rpm for 20 min at 4 °C and supernatants were run into NuPage 4–12% Bis-Tris (Life Technologies, NY) under reducing conditions. Samples were normalized based on total protein content, which was estimated by the BCA protein assay. Western blot analyses were performed using antibodies against $cPLA_2$ (sc-454 and sc-376,636,

Palavicini *et al. Acta Neuropathologica Communications* (2017) 5:56

Page 4 of 17

Santa Cruz Biotechnology -SCB-), phospho-cPLA$_2$ -S505- (2831, Cell Signaling Technology -CST-), iPLA$_2$ (sc-376,563, SCB; and NBP1–81586, Novus), MAPK p42/p44 (4695, CST), phospho-MAPK p42/p44 -T202/Y204- (4370, CST), MAPK p38 (8690, CST), phospho-MAPK p38 (rabbit polyclonal, CST), SAPK/JNK (9252, CST), active JNK (V7931, Promega), PKCα (2056, CST), PKCδ (9616, CST), PKCλ (610,207, BD Biosciences), phospho-PKC pan -βII Ser660- (9371, CST), phospho-PKCα/βII -T638/641- (9375, CST), phosphor-PKCδ -T505- (9374, CST), phospho-PKCζ/λ -T410/403- (9378, CST), CaMK2 (sc9035, SCB), pCaMK2 (sc-12,886-R, SCB), β-Tubulin (2146, CST), GAPDH (MAB374, Millipore), VDAC (4866, CST). Relative intensities were quantified using ImageJ software.

MALDI imaging

Matrix-assisted laser desorption/ionization (MALDI) imaging of fatty acids was carried out as previously described [124]. Briefly, fresh frozen brain from adult C57BL/6 J WT mouse was cryosectioned at 10-μm thickness. Brain slices were transferred onto the conductive side of indium tin oxide (ITO) slides and desiccated in vacuum for 30–60 min. After drying, N-(1-naphthyl) ethylenediamine dihydrochloride matrix was applied by the Bruker ImagePrep device (Bruker Daltonics, Bremen, Germany). MALDI mass spectra were acquired in the negative ion mode using a reflectron geometry MALDI-TOF mass spectrometer (Ultraflextreme; Bruker Daltonics) equipped with a neodymium-doped yttrium aluminum garnet (Nd:YAG)/355-nm laser as the excitation source. Imaging data were analyzed using FlexImaging v3.0 and BioMap v3.8. Ion images were generated with a bin width of ±0.2 Da. The normalization method was total ion count (TIC).

Immunofluorescence

Mouse brains were dissected, fixed in 4% paraformaldehyde, cryoprotected, embedded in OCT, and frozen. Cryostat brain sections (8 μm) were mounted on positively charged slides. Tissue-containing slides were incubated with phospho-cPLA2 -S505- (2831, CST), iPLA2 (NBP1–81586, Novus), and NeuN (NAB377, Millipore) primary antibodies overnight at 4 °C and incubated with secondary antibody (Goat anti-mouse Alexa Fluor® 555, Goat anti-rabbit Alexa Fluor® 647) for 1 h at room temperature, followed by the addition of DAPI-containing mounting media (Vectashield, Vector Laboratories). Images were taken using 20× and 40× objectives on a Nikon A1R VAAS inverted confocal microscope and analyzed using NIS-Elements imaging software (Nikon).

Statistical analysis

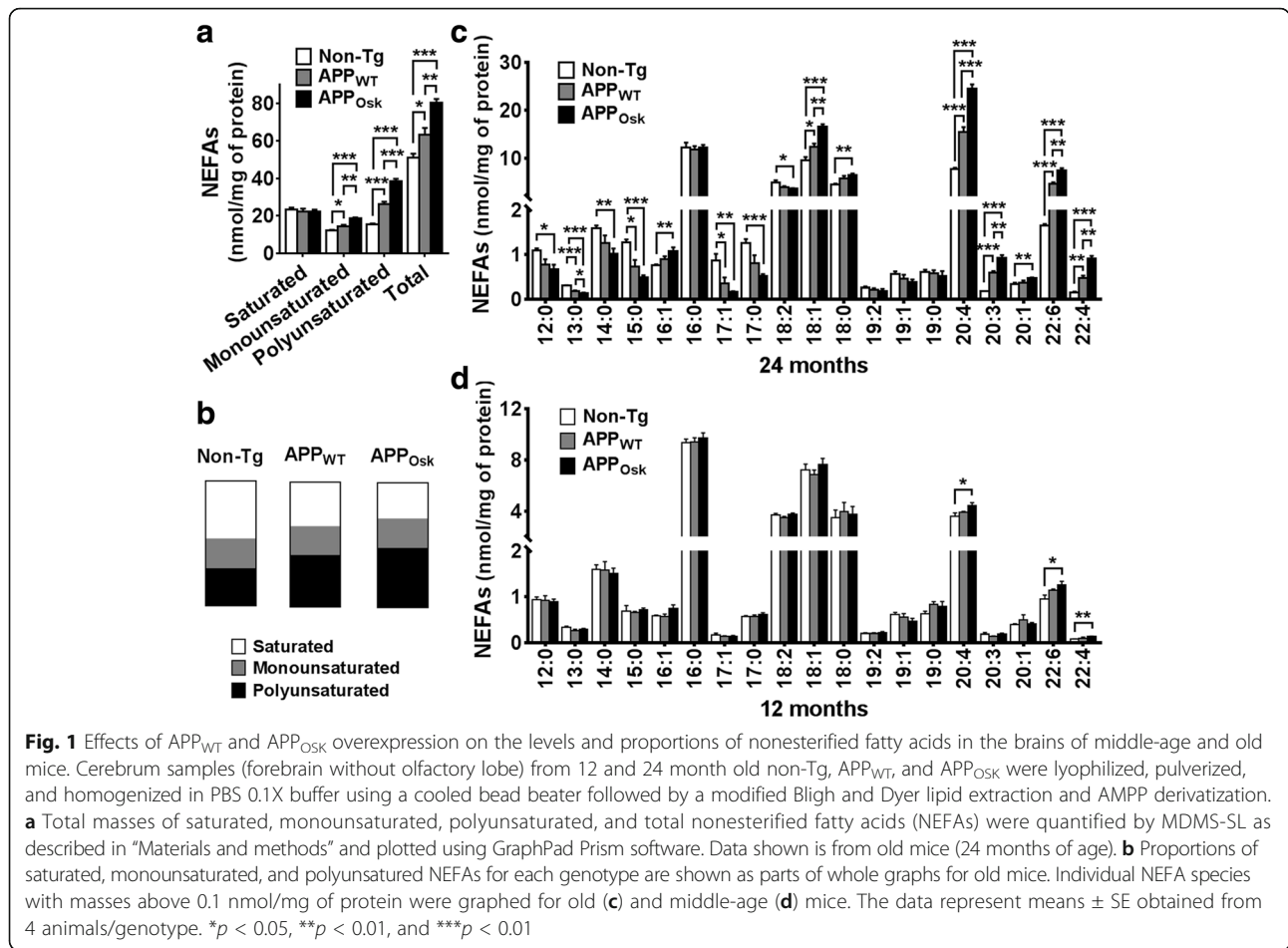Quantitative data were normalized to protein content and were presented as the means ± SE. Differences between mean values were determined by unpaired Student's *t* test (one time point analysis comparing the abundance of specific lipid species or protein between the 3 different genotypes) using GraphPad Prism software.

Results

APP overexpression and oligomeric Aβ accumulation lead to significant and additive increases in unsaturated nonesterified fatty acids

Analysis of nonesterified fatty acids (NEFAs, i.e., free FAs) within cerebrum (forebrain without olfactory lobe) homogenates from old (24-month-old) mice revealed that both APP overexpression (APP$_{WT}$) and oligomeric Aβ accumulation (APP$_{OSK}$) lead to significant and additive increases of total NEFAs (24% and 57% increase, respectively) compared to non-Tg controls (Fig. 1a). This increase occurred most dramatically within PUFAs, which increased 1.7-fold in APP$_{WT}$ and 2.5-fold in APP$_{OSK}$ mouse brains compared to non-Tg controls. Similarly, APP overexpression and high oligomeric Aβ content also led to a significant increase of monounsaturated FAs (MUFAs) (19% and 55% increase, respectively). On the other hand, the total content of saturated NEFAs was not affected either by APP overexpression or oligomeric Aβ accumulation (Fig. 1a). Consequentially, the proportion of PUFAs, which under physiological conditions (non-Tg) constitute about 30% of total NEFA content, increased to ~40% in APP$_{WT}$ and to ~50% in APP$_{OSK}$ (Fig. 1b). Conversely, the proportion of saturated NEFAs decreased from about 50% in non-Tg, to ~35% in APP$_{WT}$ and to ~30% in APP$_{OSK}$; meanwhile the proportion of MUFAs (~25%) remained unaltered between the 3 different genotypes (Fig. 1b).

Detailed characterization of NEFA molecular species of 24-month-old mice revealed that the most abundant NEFA under physiological conditions, palmitate (16:0), was not altered either by APP overexpression or oligomeric Aβ accumulation (Fig. 1c). On the other hand, under APP overexpression and oligomeric Aβ accumulation, AA (20:4) was markedly increased (2- and 3.2-fold in APP$_{WT}$ and APP$_{OSK}$, respectively), to such an extent that it became the most abundant NEFA in the brain. Importantly, altered AA metabolism has been implicated with neuroinflammation, neuronal death, and a number of neurological disorders [2, 3, 8, 31, 90, 114, 126]. Similarly, DHA (the second major PUFA in the brain) was also extensively (2.8-fold) and dramatically (4.5-fold) increased in APP$_{WT}$ and APP$_{OSK}$, respectively. It is important to note that DHA, like AA, can be metabolized by cyclooxygenase (COX) and lipoxygenase enzymes and generate active compounds [99]. DHA products, in contrast to AA products, seem to have a beneficial effect in inflammatory and neurodegenerative conditions. Thus, the increased levels of both AA and DHA in APP-Tg mice could lead to two opposite effects (pro- and anti-

Palavicini *et al. Acta Neuropathologica Communications* (2017) 5:56

Page 5 of 17

Fig. 1 Effects of APP_WT and APP_OSK overexpression on the levels and proportions of nonesterified fatty acids in the brains of middle-age and old mice. Cerebrum samples (forebrain without olfactory lobe) from 12 and 24 month old non-Tg, APP_WT, and APP_OSK were lyophilized, pulverized, and homogenized in PBS 0.1X buffer using a cooled bead beater followed by a modified Bligh and Dyer lipid extraction and AMPP derivatization. **a** Total masses of saturated, monounsaturated, polyunsaturated, and total nonesterified fatty acids (NEFAs) were quantified by MDMS-SL as described in "Materials and methods" and plotted using GraphPad Prism software. Data shown is from old mice (24 months of age). **b** Proportions of saturated, monounsaturated, and polyunsatured NEFAs for each genotype are shown as parts of whole graphs for old mice. Individual NEFA species with masses above 0.1 nmol/mg of protein were graphed for old (**c**) and middle-age (**d**) mice. The data represent means ± SE obtained from 4 animals/genotype. *$p < 0.05$, **$p < 0.01$, and ***$p < 0.01$

inflammatory, respectively). Less abundant long-chain PUFAs (like 22:4 or 20:3) were also substantially affected, showing 2- to 3-fold increases in APP_WT and 3- to 5-fold increases in APP_OSK compared to non-Tg controls. The most abundant MUFA, oleic acid (OA, 18:1), was also significantly increased (although less extensively) in both APP_WT and even further in APP_OSK mice. Less abundant MUFA species were either slightly increased only in APP_OSK mice (16:1 and 20:1), not significantly altered (19:1), or reduced (17:1) in APP-Tg mice. An additional interesting observation is that medium- and long-chain saturated NEFAs (12:0 to 15:0, and 17:0) were significantly decreased in both APP_WT and APP_OSK mice compared to controls (~30% and ~50% decrease, respectively), revealing that fatty acid metabolism undergoes significant remodeling under high APP and oligomeric Aβ content conditions (Fig. 1c).

Next, we proceeded to characterize the effects of APP_WT and APP_OSK overexpression on NEFA content in middle-aged mice (12-month-old). Although total NEFA content was not significantly altered within the brains of younger mice, the levels of the 2 major PUFAs (i.e., AA and DHA) were significantly increased in APP_OSK mice compared to

non-Tg controls (~20% and ~30% increase, respectively); while saturated and monounsaturated NEFAs were not significantly altered in middle-aged mice (Fig. 1d).

As expected, ELISA analysis (using 11A1, an antibody against human oligomeric Aβ) revealed an age dependent increase of oligomeric Aβ content in APP_OSK mice, which accumulated higher levels of oligomeric Aβ than APP_WT controls (Fig. 2a). These results are consistent with previous reports, where high levels of human oligomeric Aβ have been reported in the brains of APP_OSK mice compared to APP_WT controls or non-Tg (which lack human Aβ) by Western blot, ELISA, and immunohistochemistry [115, 118].

APP overexpression and oligomeric Aβ accumulation lead to a significant and additive increase of lysoPC content

The dramatic increases in long-chain PUFAs (particularly AA and DHA) on transgenic APP mice were strongly suggestive of increased PLA_2 activity; thus, we proceeded to characterize the content of brain lysophospholipids (LPLs) in old and middle-age mice. As expected from the NEFA results, we observed an upward trend in total lysoPC in 24-month-old APP_WT mice (15%) and a significant increase in

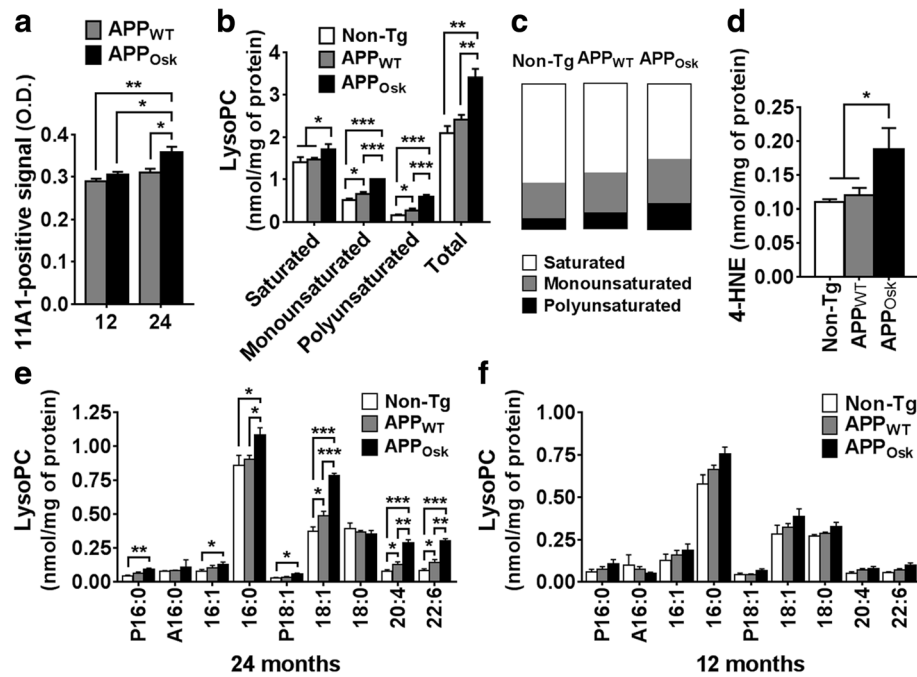Palavicini *et al. Acta Neuropathologica Communications* (2017) 5:56

Page 6 of 17

Fig. 2 Age-dependent effects of oligomeric Aβ accumulation in APP$_{WT}$ and APP$_{OSK}$ mouse brains on the levels and proportions of lysophosphatidylcholines and 4-HNE. Cerebrum samples from 12 and 24 month old non-Tg, APP$_{WT}$, and APP$_{OSK}$ were lyophilized, pulverized, and homogenized in PBS 0.1X buffer using a cooled bead beater followed by a modified Bligh and Dyer lipid extraction. **a** PBS supernatants were subjected to direct oligomer Aβ -11A1- ELISA, O.D. values are shown. **b** Total masses of saturated, monounsaturated, polyunsaturated, and total lysophosphatidylcholines (lysoPCs) for old mice were quantified by MDMS-SL as described in "Materials and methods" and plotted using GraphPad Prism software. **c** Proportions of saturated, monounsaturated, and polyunsaturated lysoPCs for each genotype are shown as parts of whole graphs. **d** Total 4-HNE content in 24-month old mice. Individual lysoPC species with masses above 0.05 nmol/mg were graphed for old −24 months- (**e**) and middle-age − 12 months- mice (**f**). The data represent means ± SE obtained from 4 animals/genotype. *$p < 0.05$, **$p < 0.01$, and ***$p < 0.01$

APP$_{OSK}$ mice (63%) compared to non-Tg controls (Fig. 2b). PLA$_2$ cleavage results in lysoPL molecular species containing a FA in the *sn*-1 position, which is typically occupied by saturated or MUFAs. Consistently, the levels of lysoPC containing a saturated FA increased in APP$_{OSK}$ mice compared to APP$_{WT}$ and non-Tg mice. Furthermore, the levels of lysoPC containing a MUFA were significantly and additively increased in APP$_{WT}$ and APP$_{OSK}$ (by 30% and 98%, respectively). Unexpectedly, the levels of lysoPC containing PUFAs were also significantly and additively increased in APP$_{WT}$ and APP$_{OSK}$ (1.7- and 3.7-fold increases, respectively, Fig. 2b).

The unexpected increase in PUFA-containing lysoPC in APP-Tg mice could theoretically be explained by (1) a higher proportion of PUFAs at the *sn*-1 position, (2) increased PLA$_1$ activity, and/or (3) increased reactive oxygen species (ROS)-mediated lysoPC formation under pathological conditions (in APP-Tg mice). The fact that PUFA-containing lysoPCs constitute only a minority of the total lysoPCs (8%, 11%, and 18% in non-Tg, APP$_{WT}$ and APP$_{OSK}$, respectively, Fig. 2c) supports the notion that PLA$_2$ activity in the brain is dominant over PLA$_1$ under physio(patho)logical conditions and that PUFAs

are preferentially located at the *sn*-2 position. Therefore, we propose that the increase in PUFA-containing lysoPCs is most likely due to high ROS production under high oxidative stress pathogenic conditions (APP$_{WT/OSK}$ overexpression). Increased lysoPL, particularly those containing PUFAs at the *sn*-2 position resulting from plasmalogen (*sn*-1) phospholipid cleavage, is a well stablished oxidative stress signature [10, 33, 42, 51]. Consistent with our proposed model, we found that the levels of 4-hydroxynonenal (4-HNE), a product of oxidative stress induced lipid peroxidation, were significantly increased in APP$_{OSK}$ mice compared to APP$_{WT}$ and non-Tg controls (by 66%, $p = 0.04$) (Fig. 2d). In agreement with our data, increased ROS-generation has been reported in APP$_{OSK}$ expressing COS-7 cells [84] and Aβ oligomers have been shown to induce neuronal oxidative stress [27].

Detailed characterization of lysoPC lipid species revealed that plasmalogen palmitic (P16:0), palmitoleic (16:1), and oleic acid (P18:1 and 18:1) containing lysoPC species were significantly and similarly increased (by 1.7- to 2.2-fold) in old APP$_{OSK}$ mice compared to non-Tg controls. Similarly, these species (*sn*-1 lysoPCs) either showed an upward trend or were significantly and similarly increased in old APP$_{WT}$

Palavicini *et al. Acta Neuropathologica Communications* (2017) 5:56

Page 7 of 17

mice (1.3- to 1.5-fold) (Fig. 2e). On the other hand, AA and DHA containing lysoPC species (*sn*-2 lysoPCs) were more extensively increased in APP_{WT} (by 1.7-fold) and in APP_{OSK} mice (by almost 4-fold) compared to non-Tg controls. The difference in the extent of increase in *sn*-1 versus *sn*-2 lysoPCs is consistent with two different processes responsible for their altered levels (PLA$_2$ activity versus ROS-mediated oxidation, respectively).

Next, we proceeded to characterize the effects of APP_{WT} and APP_{OSK} overexpression on lysoPC content in middle-aged mice (12-month-old). Consistent with our NEFA data, total lysoPC content was not significantly altered within the brains of younger mice (Fig. 2f). Detailed analysis of lysoPC species revealed that APP_{OSK} tended to have higher levels of the same species that accumulated in old animals, although these increases were not statistically significant (Fig. 2f). Finally, it is important to mention that we also measured lysoPE content; however, no significant changes were detected between the total levels of the 3 analyzed mouse genotypes within middle-aged or old mice (data not shown). These results are consistent with previous reports claiming that cPLA$_2$α is selective for AA-containing phosphatidylcholine (PC) [81].

APP overexpression and oligomeric Aβ accumulation lead to dysregulation of cPLA$_2$.

Our NEFA and lysoPC results strongly suggested that APP overexpression and oligomeric Aβ lead to increased PLA$_2$ activity. Thus, we proceeded to characterize the major brain PLA$_2$ isoforms by Western blot (WB). Specifically, we focused on characterizing cPLA$_2$ (GIV) and iPLA$_2$ (GVI), given that sPLA$_2$ (GIIA) is absent in the APP-Tg and non-Tg mice used because of a frame-shift mutation in exon 3 in the C57BL6 strain [54].

Intriguingly, even though the molecular weight of cPLA$_2$α is 85 kDa, published SDS-PAGE-based WB studies have reported cPLA$_2$α signals that range from 85 to 120 kDa [7, 20, 59]. We used 3 different cPLA2 antibodies purchased from 2 different companies (Cell Signaling and Santa Cruz) and observed 3 different bands (115 kDa, 120 kDa, and 85 kDa) depending on which antibody was used (Fig. 3a). The antibody from Cell Signaling recognized a previously described non-phosphorylated ~115 kDa cPLA$_2$α band, which under physiological conditions appeared as the most intense band. An additional and previously described phosphorylated ~120 kDa cPLA$_2$α band was also observed. Importantly, both of this bands were shown to be specific to cPLA$_2$α since they were absent in cPLA$_2$α KO mice. Longer exposure times revealed an additional ~85 kDa band (not shown). Interestingly, characterization of 2 different Santa Cruz antibodies (recognizing either cPLA$_2$ N- or C-terminus) failed to detect the 115 and 120 kDa bands but effectively detected the 85 kDa band. Long
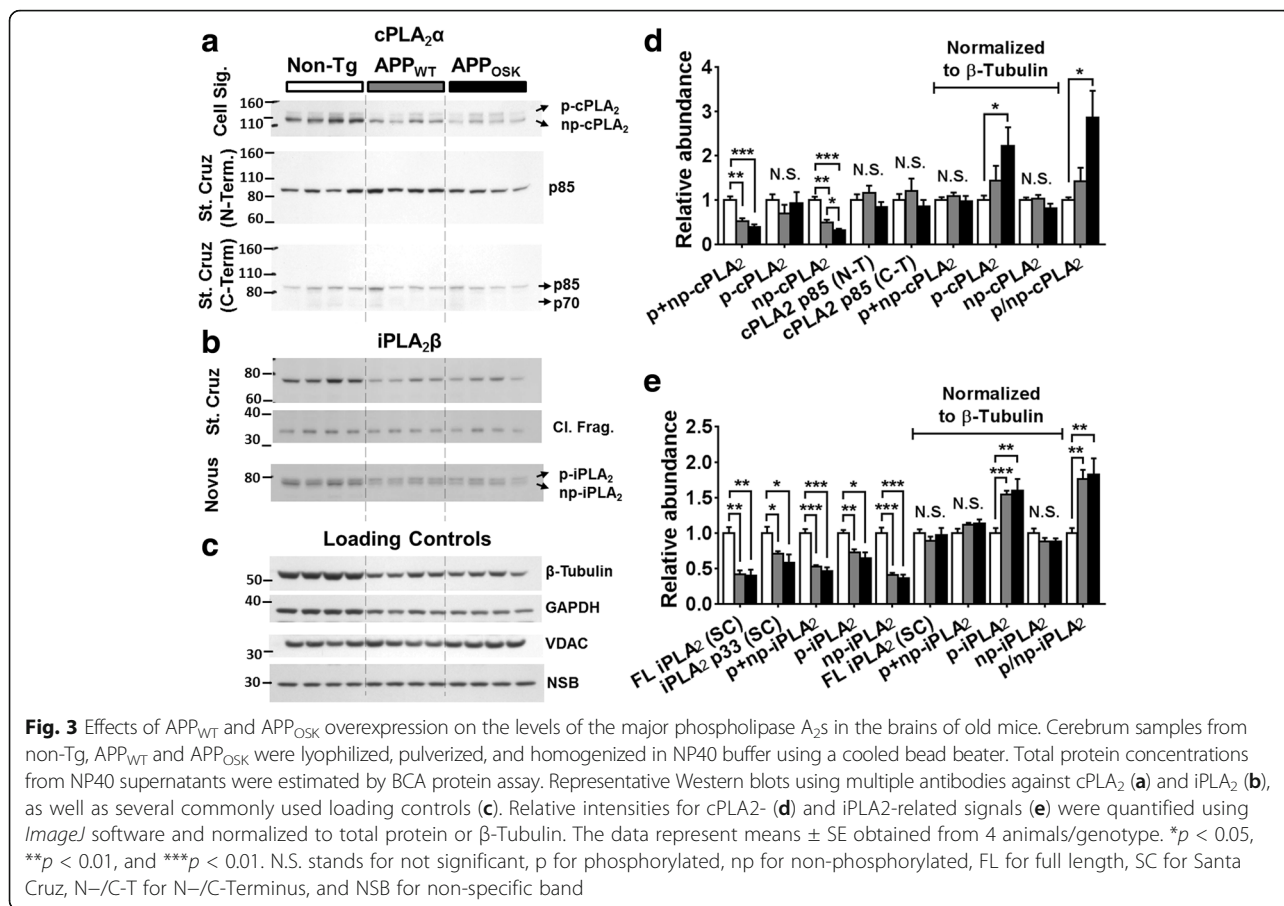
exposures of the antibody against C-terminus cPLA$_2$ (H-12, sc-376,636) also revealed a weak previously reported 70 kDa cPLA$_2$ cleavage product band (Fig. 3a).

Unexpectedly, WB analysis of cPLA$_2$α revealed a significant decrease of total cPLA$_2$α levels (phospho + nonphosphorylated or 115 + 120 kDa bands) in both old APP_{WT} (reduced by 48%) and APP_{OSK} mice (reduced by 61%) compared to non-Tg controls (Fig. 3a and d) after normalizing to total protein or certain loading controls (like VDAC or COX IV). Surprisingly, several commonly used loading controls (like β-Tubulin, GAPDH and PCNA) were also significantly reduced in APP-Tg mice (Fig. 3c). These decreases paralleled the reductions observed in total cPLA$_2$, in fact, if normalized against any of these common loading controls, total cPLA$_2$ levels were not altered (Fig. 3d). Consistently with our lipidomics data, we observed a significant increase (2.9-fold) in the ratio of phospho- to non-phospho-cPLA$_2$ in old APP_{OSK} mice and an upward trend (1.4-fold) in APP_{WT} mice compared to non-Tg controls (Fig. 3a and b). On the other hand no significant changes in the levels of the 85 kDa band were detected in any of the 3 antibodies used after normalizing to total protein or VDAC (Fig. 3a and d). The previously reported 70-kDa cPLA$_2$ fragment [1, 5, 6, 30, 40, 119, 128] was very weak within all of the homogenates. The fact that this cleavage fragment did not accumulate in APP-Tg mice clarifies that the decrease in total cPLA$_2$ is not a consequence of increased proteolytic cleavage.

APP overexpression leads to dysregulation of iPLA$_2$

Given that iPLA$_2$ has been proposed to be highly specific to DHA cleavage/release [37, 69], to be enriched in AD-vulnerable brain regions (cortex and hippocampus) [87, 132], and to account for more than 70% of the brain PLA$_2$ activity [132], we reasoned that the increases of free DHA found in our lipidomics analysis were likely due to the increased activity of iPLA$_2$ in APP-Tg mice.
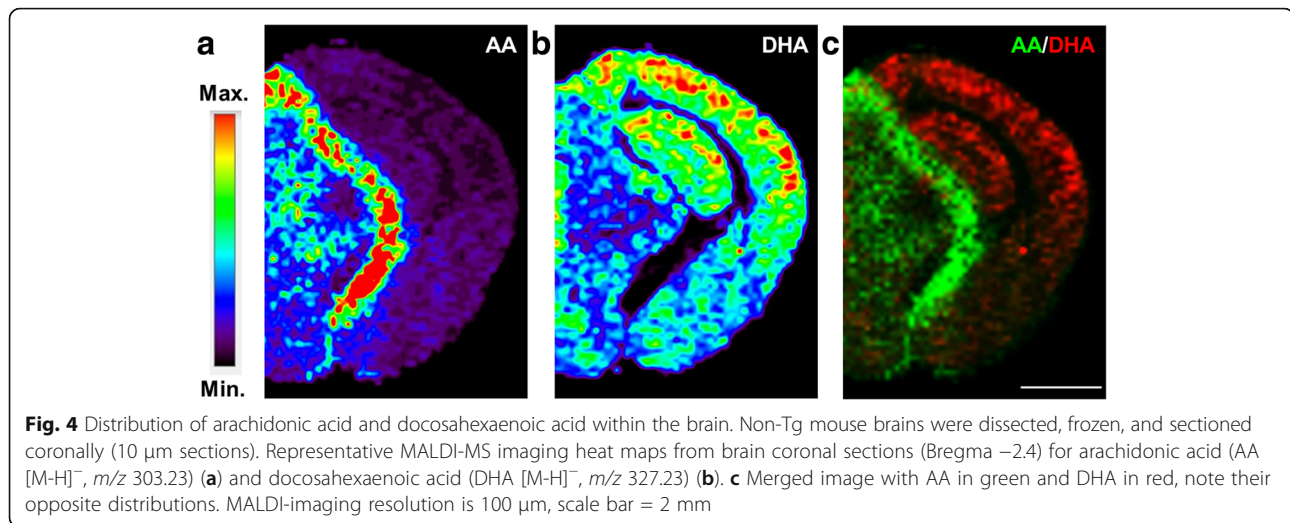
Surprisingly, as for cPLA$_2$α, WB analysis revealed reduced levels of total iPLA$_2$β (~78 kDa) in APP-Tg mice (60% reduction in both APP_{WT} and APP_{OSK}) compared to non-Tg controls (Fig. 3b and e) after normalizing to total protein and/or certain loading controls (e.g., VDAC). Again, total iPLA$_2$ levels paralleled the levels of several commonly used loading controls (e.g., β-Tubulin), so that if normalized against any of them, total iPLA$_2$ levels were not altered (Fig. 3b and e). Importantly, our WB analyses were confirmed using two different iPLA$_2$β antibodies (Novus and Santa Cruz) that target different epitopes (near the N- and C-terminus, respectively). Notably, one of the antibodies (N-terminus) yielded an additional band right above the band corresponding to full length (FL) iPLA$_2$β (~80 kDa). It is reasonable to speculate that this additional band could represent phosphorylated iPLA$_2$β. Importantly, the ratio of this putative phosphorylated

Palavicini *et al. Acta Neuropathologica Communications* (2017) 5:56

Page 8 of 17

Fig. 3 Effects of APP_{WT} and APP_{OSK} overexpression on the levels of the major phospholipase A_2s in the brains of old mice. Cerebrum samples from non-Tg, APP_{WT} and APP_{OSK} were lyophilized, pulverized, and homogenized in NP40 buffer using a cooled bead beater. Total protein concentrations from NP40 supernatants were estimated by BCA protein assay. Representative Western blots using multiple antibodies against $cPLA_2$ (**a**) and $iPLA_2$ (**b**), as well as several commonly used loading controls (**c**). Relative intensities for cPLA2- (**d**) and iPLA2-related signals (**e**) were quantified using *ImageJ* software and normalized to total protein or β-Tubulin. The data represent means ± SE obtained from 4 animals/genotype. *$p < 0.05$, **$p < 0.01$, and ***$p < 0.01$. N.S. stands for not significant, p for phosphorylated, np for non-phosphorylated, FL for full length, SC for Santa Cruz, N–/C-T for N–/C-Terminus, and NSB for non-specific band

$iPLA_2\beta$ to non-phosphorylated $iPLA_2\beta$ was significantly increased in APP-Tg mice compared to non-Tg controls (Fig. 3e). Consistently with the literature [136], we did find a ~ 33 kDa C-terminal fragment (when using the antibody against the C-terminal region of $iPLA_2\beta$) (Fig. 3b and e). This cleaved $iPLA_2\beta$ fragment was significantly reduced in APP-Tg mice (by 30% and 42% in APP_{WT} and APP_{OSK}, respectively). However, this decrease was mild compared to the more extensive reduction in FL $iPLA_2\beta$. Consequentially, cleaved to FL ratios were significantly higher (50–70%, $p < 0.05$) in APP-Tg mice compared to non-Tg controls. These results suggest that under APP overexpressing conditions, FL $iPLA_2\beta$ is more likely to be processed than under physiological conditions. Nevertheless, increased FL $iPLA_2\beta$ cleavage ratios in APP-Tg mice do not fully explain the reduction of total $iPLA_2\beta$ (in which case the cleaved fragment would accumulate). Given that the reduction of total levels of $iPLA_2$ paralleled the reduction seen for $cPLA_2$, and "housekeeping" gene products (i.e., β-Tubulin, GAPDH, PCNA, and others), it seems likely that these decreases must be due to a more global effect (e.g., reduced expression of certain gene products or reduced density of certain cell types).

DHA and AA accumulate in different and opposite brain regions

Given the opposite effects of AA and DHA (pro- and anti-inflammatory, respectively), we wondered whether their distribution in the brain would also differ under physiological conditions. Interestingly, MALDI-MS imaging analysis revealed that AA and DHA accumulated in different and opposite brain regions (Fig. 4). Imaging analysis of coronal sections revealed that AA signals were highest along the brachium of the superior colliculus and optic tract, while mild signals were seen within thalamic and hypothalamic regions, and low or virtually no signals were observed within the amygdala and cortical/hippocampal regions (Fig. 4a). On the other hand, DHA signals were highest within the cortex and hippocampus, while mild signals were seen within the amygdala, and low signals were detected within thalamic and hypothalamic regions (Fig. 4b). In summary, AA seems to concentrate along bundles of nerve fibers while DHA is most abundant within regions rich in pyramidal neurons. Thus, AA and DHA not only have opposing signaling effects, but they also have opposite distributions throughout the brain.

Palavicini *et al. Acta Neuropathologica Communications* (2017) 5:56

Page 9 of 17

Fig. 4 Distribution of arachidonic acid and docosahexaenoic acid within the brain. Non-Tg mouse brains were dissected, frozen, and sectioned coronally (10 μm sections). Representative MALDI-MS imaging heat maps from brain coronal sections (Bregma −2.4) for arachidonic acid (AA [M-H]⁻, m/z 303.23) (**a**) and docosahexaenoic acid (DHA [M-H]⁻, m/z 327.23) (**b**). **c** Merged image with AA in green and DHA in red, note their opposite distributions. MALDI-imaging resolution is 100 μm, scale bar = 2 mm

Spatial distribution of cPLA$_2$ and iPLA$_2$ in the brain

We speculated that cPLA$_2$ and iPLA$_2$ should be expressed in different brain regions explaining the opposed distribution patterns observed for DHA and AA. Immunohistochemical analysis revealed that cPLA$_2$ staining was most intense within regions rich in white matter tracts as well as within the thalamus and hypothalamus (Fig. 5a, left). In fact, cPLA$_2$ staining highly resembled the typical staining of myelin-specific proteins. On the other hand iPLA$_2$ staining was most intense within the hippocampus, while significant signals were also observed within thalamic, cortical, and amygdala regions (Fig. 5b, left). Contrary to cPLA$_2$ staining, iPLA$_2$ signals were virtually absent within white matter tracks (e.g., corpus callosum, CC). More detailed characterization at higher magnifications revealed that cPLA$_2$ was enriched within the CC and at the border between hippocampal strata radiatum (Rad) and lacunosum moleculare (LM) (Fig. 5a, middle). cPLA$_2$ signals were specific to myelinated axons and virtually absent in neuronal cell bodies (Fig. 5a, right). On the other hand, the strongest iPLA$_2$ signal was found within neuronal cell bodies of the stratum pyramidale (Py) of the hippocampus. Interestingly, iPLA2 staining colocalized with NeuN (a pan neuronal marker) staining only within pyramidal neurons, and not within interneurons or granule cells of the dentate gyrus. In addition, iPLA$_2$ was also observed within regions of dendritic arborization (e.g., Rad) (Fig. 5b, right). Similarly, iPLA$_2$ and NeuN co-staining was also observed within pyramidal neurons in the cortex and amygdala (not shown at high magnification).

Unraveling the kinases responsible for inducing iPLA$_2$ phosphorylation in APP-Tg mouse brain tissue

To further confirm and better understand the mechanisms leading to cPLA$_2$ and/or iPLA$_2$ activation in APP-Tg mice, we proceeded to examine the kinases that have been demonstrated to phosphorylate cPLA$_2$ as well as putative kinases that may phosphorylate iPLA$_2$. Previous studies have shown that phosphorylation of cPLA$_2\alpha$ by mitogen-activated protein kinase (MAPK) (p42/44 and p38) at Ser505 and by Ca^{2+}/calmodulin-dependent protein kinase II (CaMKII) at Ser515 stimulate its catalytic activity [34, 50, 60, 66]. Finally, it has also been shown that okadaic acid activates cPLA$_2\alpha$ and stimulates AA release via a p54 kinase [117].

We decided to characterize the 3 classical MAPK families: p38, p44/p42 (also known as ERK1/2), and JNK1/2 since the first two have been shown to directly phosphorylate cPLA$_2$ and the fact that JNK2 has a molecular weight of 54 kDa. MAPKs are catalytically inactive in their base form and activated by phosphorylation (within residues of their activation loops). Thus, WB analysis using both total and phospho-specific antibodies provides a straightforward means to estimate their relative activities under different conditions (calculated as phospho- to total MAPK ratios). As expected from our lipidomics and PLA$_2$ WB analyses, we found that APP-Tg mice showed increased MAPK activities (i.e., higher phospho/total MAPK ratios) compared to non-Tg controls (Fig. 6a-c and e). These significant increases were most dramatic for p42, where phospho/total ratios were 6-fold higher in APP$_{WT}$ and 13-fold higher in APP$_{OSK}$ compared to non-Tg controls (Fig. 6b and e). Phospho/total JNK1/2 ratios were also extensively increased in APP-Tg mice (4 to 5-fold and 6 to 9-fold increases in APP$_{WT}$ and APP$_{OSK}$, respectively) (Fig. 6c and f). Similarly, phospho/total p44 ratios were 2- and 3-fold higher in APP$_{WT}$ and APP$_{OSK}$ (Fig. 6b and e); while the phospho/total p38 MAPK ratios were mildly but significantly increased in APP-Tg mice (by 50% and 70% in APP$_{WT}$ and APP$_{OSK}$, respectively) (Fig. 6a and e).
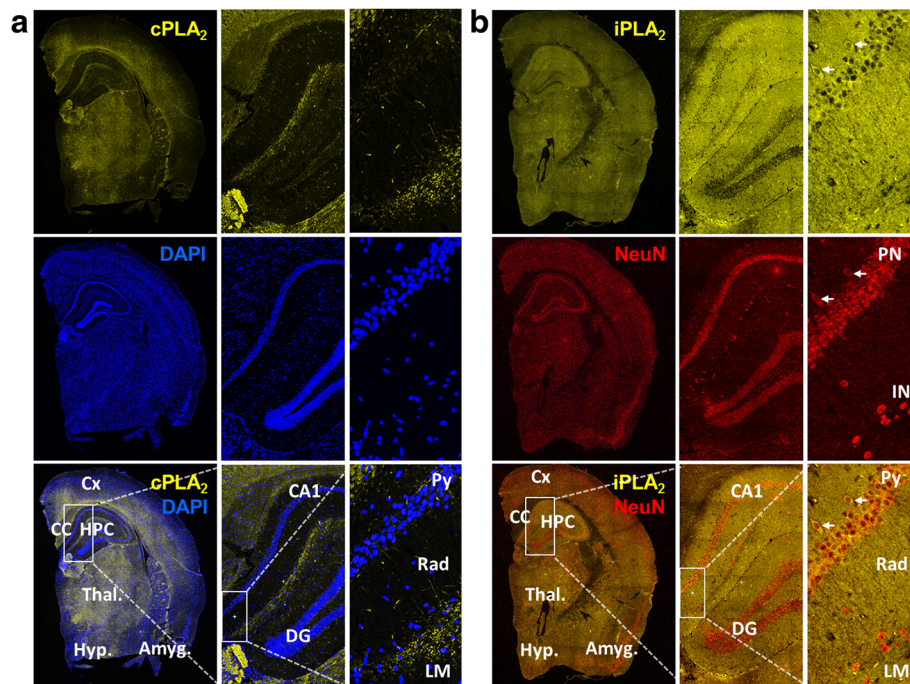
Palavicini *et al. Acta Neuropathologica Communications* (2017) 5:56

Page 10 of 17

Fig. 5 Distribution of cPLA$_2$ and iPLA$_2$ within the brain. Non-Tg mouse brains were dissected, fixed in 4% paraformaldehyde, cryoprotected, frozen, and sectioned coronally (8 μm sections). Representative immunofluorescence images were taken from brain coronal sections (Bregma −2) using phospho-cPLA$_2$ (yellow) antibody and DAPI (blue) (**a**) or and iPLA$_2$ (yellow) and NeuN (red) antibodies (**b**). The images show a whole hemibrain section using a 20× objective on a Nikon A1R VAAS inverted confocal (left panels in *A* and *B*). Cortex (Cx), corpus callosum (CC), hippocampus (HPC), thalamus (Thal.), hypothalamus (Hyp.), and amygdala (Amyg.). A zoom to hippocampal CA1/dentate gyrus (DG) (middle panels in **a** and **b**), and a zoom to the strata pyramidale (Py), radiatum (Rad) and lacunosum moleculare (LM) (right panels in **a** and **b**) were taken using a 40× objective. Note the clear axonal cPLA$_2$ staining within myelin-rich regions and its absence within the cell bodies or dendritic arborization of pyramidal neurons (right panels, **a**). NeuN and iPLA$_2$ co-localize within the perinucleus of pyramidal neurons (PN, white arrows), but not within the perinucleus of interneurons (IN). iPLA$_2$ staining is also observed within pyramidal dendritic arborization (right panels, **b**)

Next, we proceeded to measure the levels of phospho- to total CaMKII since it has also been shown to phosphorylate cPLA$_2$ at a different residue (S515). However, we did not find any significant differences in phospho/ total CaMKII ratios between APP-Tg and non-Tg mice (Fig. 6d and f), suggesting that activation of cPLA$_2$ by phosphorylation in APP-Tg mice occurs via the MAPK, but not the CaMK2 pathway. It is important to mention that as for cPLA$_2$ and iPLA$_2$, the levels of total CaMKII were significantly reduced in aged APP-Tg mice compared to non-Tg controls. Again, this decrease paralleled those seen for typical "loading control" proteins. On the other hand, MAPKs were not significantly decreased in APP-Tg mice. Finally, analysis of middle-age mice revealed no significant differences in the levels of the analyzed phospho- or total kinases (data not shown), consistently with our lipidomics and PLA$_2$ data.

MAPK activation occurs independently of PKC activation in aged APP-Tg mice

We proceeded to assess whether MAPK activation occurred in a PKC-dependent manner in APP-Tg mice.

For this purpose, we characterized multiple isoforms of conventional, novel, and atypical PKCs as well as different phosphorylation events (at the activation loop, turn motif, and hydrophobic motif of PKCs) that have been linked to increased PKC activity [55]. Total levels of conventional PKCα were not altered between APP-Tg and non-Tg mice, while the levels of phospho-PKCα/βII (T638/641) (autophosphorylation event at the turn motif) were actually slightly reduced in APP-Tg mice compared to non-Tg controls. Total levels of novel (δ) and atypical (ζ/λ) PKCs were extensively reduced in APP-Tg mice compared to non-Tg controls (Fig. 7a-b). Interestingly, the total levels of novel and atypical PKCs paralleled those observed for total PLA$_2$s and commonly used loading controls. Similarly, phosphorylation levels of novel (δ) and atypical (ζ/λ) PKCs at the activation loop (T505 and T410/ 403, respectively) were also extensively reduced in APP-Tg mice compared to non-Tg controls (Fig. 7a-b). Therefore, phospho/total novel/atypical PKC ratios were not significantly altered between the 3 genotypes. Finally, we also characterized the final PKC autophosphorylation event at the hydrophobic motif which represents the third
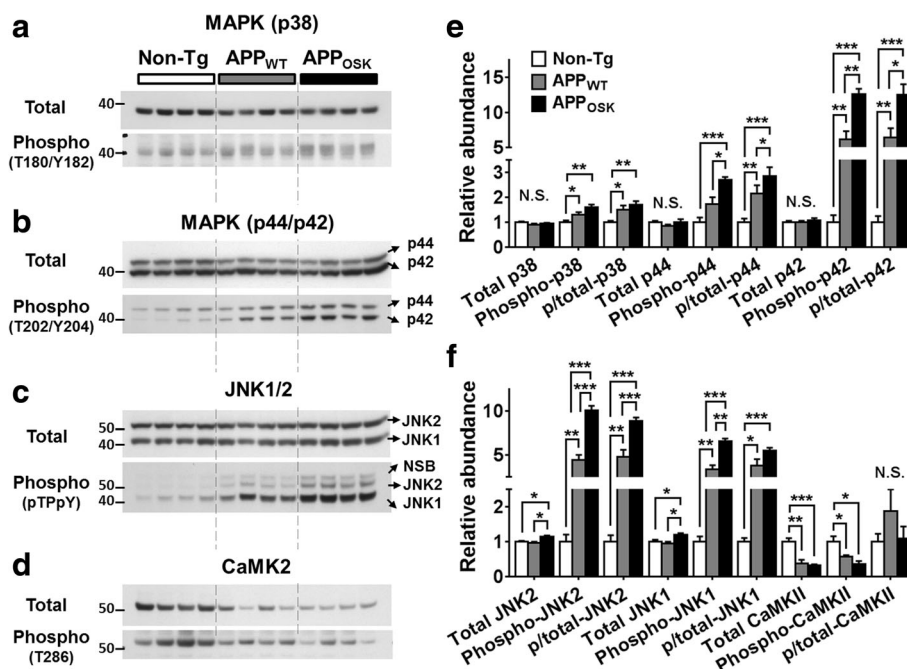
Palavicini *et al. Acta Neuropathologica Communications* (2017) 5:56

Page 11 of 17

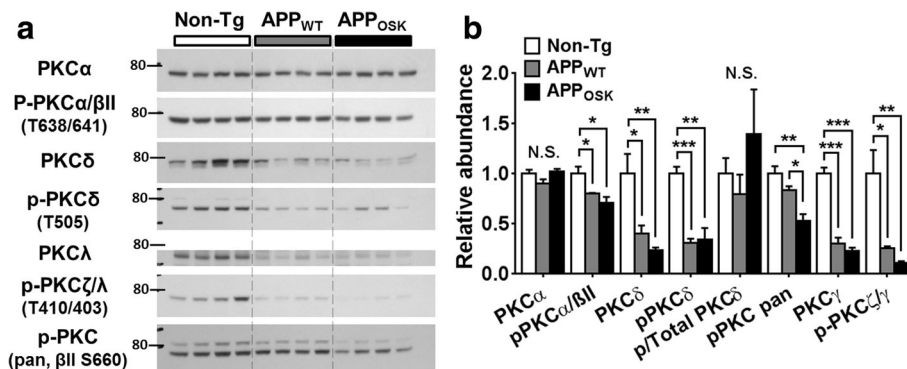**Fig. 6** Effects of APP_WT and APP_OSK overexpression on the levels of known PLA_2 kinases in the brains of old mice. Cerebrum samples from non-Tg, APP_WT, and APP_OSK were lyophilized, pulverized, and homogenized in NP40 buffer using a cooled bead beater. Total protein concentrations from NP40 supernatants were estimated by BCA protein assay. Representative Western blots using antibodies against total and phospho-MAPK p38 (**a**), p44/p42 (**b**), JNK1/2 (**c**), and CaMK2 (**d**). **e-f** Relative intensities were quantified using *ImageJ*. The data represent means ± SE obtained from 4 animals/genotype. *$p < 0.05$, **$p < 0.01$, ***$p < 0.01$, and N.S. as for not significant

and last phosphorylation/activation step using phospho-PKC (pan) (βII S660) against all conventional and novel PKCs. Consistently with the results obtained from the other 2 phosphorylation sites analyzed, we also observed a significant reduction of phosphorylation levels at this position (Fig. 7a-b). Thus, after analyzing multiple PKC isoforms and phosphorylation events, we did not find any evidence of PKC activation in APP-Tg mice.

Discussion

Seeking to better understand the role of fatty acid metabolism in AD and to unravel the mechanisms underlying its disruption we took advantage of the powerful technology of multidimensional mass spectrometry-based shotgun lipidomics (MDMS-SL) pioneered by our laboratory. At the same time, attempting to dissect if fatty acid dysregulation is linked to fibrillar and/or soluble Aβ accumulation, we took

Fig. 7 Effects of APP_WT and APP_OSK overexpression on the levels of total and phosphorylated PKCs in the brains of old mice. Cerebrum samples from non-Tg, APP_WT, and APP_OSK were lyophilized, pulverized, and homogenized in NP40 buffer using a cooled bead beater. **a** Representative Western blots using antibodies against total and phospho-PKC isoforms. **b** Relative intensities were quantified using *ImageJ*. The data represent means ± SE obtained from 4 animals/genotype. *$p < 0.05$, **$p < 0.01$, ***$p < 0.01$, and N.S. as for not significant

advantage of the APP_{OSK} mouse model where AD-like pathology and neurodegeneration occur as a consequence of high levels of soluble oligomeric Aβ in the absence of amyloid plaques. Importantly, besides non-Tg control mice, our studies also included APP_{WT} transgenic controls; this experimental design allowed us to distinguish between the effects of APP overexpression and those of oligomeric Aβ accumulation. To the best of our knowledge, this is the first study to demonstrate that (1) dysregulation of fatty acid metabolism in the context of AD occurs independently of amyloid plaques, (2) APP overexpression on its own induces an accumulation of unsaturated NEFAs (particularly AA, DHA, and OA) and lysoPCs while soluble oligomeric Aβ further exacerbates this accumulation of unsaturated FAs/lysoPCs, (3) cPLA2/AA and iPLA2/DHA accumulate in different and opposite brain regions, (4) AD-related fatty acid dysregulation is induced by PLA_2 activation via MAPK-mediated phosphorylation in a PKC-independent manner.

Fatty acid metabolism disruption in AD is mediated by increased PLA_2 activity

Thanks to the fact that disruption of fatty acid metabolism results in specific signatures within the lipidome (depending on whether the alterations are induced through biosynthesis and/or degradation pathways), our lipidomics approach enabled us to not only demonstrate that both APP overexpression and high oligomeric Aβ content lead to significant and additive increases in unsaturated NEFAs within the brain of aged mice, but also to gain insights into the mechanisms underlying this disruption of FA metabolism. The lipidomics signature obtained strongly indicated that the accumulation of NEFA occurred as a consequence of increased FA cleavage. Specifically, analysis of the two major lysophospholipids classes revealed a dramatic accumulation of lysoPCs. Detailed characterization of specific lysoPC species indicated that FA cleavage in the context of AD seems to be induced by increased PLA_2 activity as well as oxidative stress (revealed by an accumulation of 4-HNE and *sn*-2 lysoPCs). We validated this lipidomics-based hypothesis by analyzing the most abundant PLA_2 enzymes in the brain by WB and provided evidence supporting a model in which increased PLA_2 activity is mediated by phosphorylation of cPLA₂α and iPLA₂β.

These results are in agreement with multiple previous reports linking high AA content and $cPLA_2$ activity/phosphorylation to AD (reviewed in [94]) [22, 95, 108, 109, 111, 113]. Furthermore, two separate groups have recently reported increased free DHA levels in human AD brains [82, 105]. In addition, the proportion of phospholipid-bound DHA has been reported to be decreased in AD brains [25], which is also consistent with increased FA cleavage rates. The fact that $iPLA_2$ has been shown to preferentially cleave/release DHA from brain phospholipids [37, 69] together with our

data from AD mice and human data from other labs showing increased levels of free DHA, strongly implicate $iPLA_2$ as a potential driver of this accumulation. To the best of our knowledge we are the first ones to propose an association between iPLA₂β and AD.

Taken together our results strongly suggest that both PLA_2-mediated accumulation of free PUFAs and oxidative stress drive AD-related disruption of lipid metabolism. Furthermore, we think that oligomeric Aβ-induced NEFA accumulation might be associated with the "adipose inclusions" described by Alois Alzheimer more than a century ago.

Opposite brain spatial distribution between cPLA₂/AA and iPLA₂/DHA

In vitro studies have shown that cerebral microvascular endothelium and astrocytes can produce DHA and AA [76, 77]; in contrast, neurons cannot produce PUFAs but get enriched with PUFAs if they are co-cultured with astrocytes and endothelial cells. Interestingly, MALDI-MS imaging analysis revealed that AA and DHA accumulate within different and opposite brain regions. We found that although free DHA is detected throughout the brain, it accumulates most strongly within cortical and hippocampal regions, both of which are rich in pyramidal neurons/dendritic spines and are severely affected in AD. Consistent with this observation, previous studies have reported that 50% of the weight of neuronal plasma membrane is composed by DHA [103, 121]. Our results suggest that even under physiological conditions, there is a high exchange between free and lipid-bound DHA, presumably due to the high levels of plasma membrane remodeling that occur within dendritic spines (which are particularly enriched in pyramidal neurons). On the other hand, AA levels were strongest along bundles of nerve fibers and moderate within thalamic and hypothalamic regions, while cortical and hippocampal regions showed negligible levels of AA. It is reasonable to speculate that the opposite localization of free AA and DHA within the brain could be evolutionarily related to their opposite roles as mediators of pro- and anti-inflammatory signaling pathways.

Given that epidemiological research has linked high DHA consumption with a lower risk of AD [79] and animal studies have reported a reduction of amyloid, tau, and neuritic pathology with oral intake of DHA [12, 38, 65], it could seem paradoxical that AD brains accumulate free DHA. However, it is important to consider that DHA consumption is likely to result in increased membrane-associated (lipid-bound) DHA content which is of structural and functional relevance; while phospholipid cleavage under pathological conditions is likely to result in reduced lipid-bound DHA and increased free DHA. In fact, in AD there is a dramatic loss of dendritic spines as well as a significant loss of neurons with a concomitant increase in the levels of astrocytes (reviewed

Palavicini *et al. Acta Neuropathologica Communications* (2017) 5:56

Page 13 of 17

in [58, 91]). This cell-type remodeling could explain the overall increase in free PUFAs reported here and by others [82, 105].

Supporting our proposed model in which iPLA$_2$ activation induces free DHA accumulation, we observed a strong correlation between DHA MALDI-imaging maps and iPLA$_2$ immunofluorescence. Specifically, we report iPLA$_2$ immunolabeling within the perinuclear cytoplasm and dendritic arborization of pyramidal neurons. Importantly, these results are in agreement with a previous study that reported high iPLA$_2$ expression within the hippocampus (i.e. in the nuclear envelope of neurons, dendrites, and axon terminals) and lower expressions within the thalamus and hypothalamus of monkey brains [87].

On the other hand, AA and cPLA$_2$ histological studies also revealed an overlap in their localizations. Specifically, both AA and cPLA$_2$ accumulated within nerve fiber bundles and showed significant levels within thalamic and hypothalamic regions, revealing that cPLA$_2$ and AA release are highly specific to myelin-rich regions. Previous characterization of cPLA$_2$ within the rat brain noted high activities and immunoreactivities in the hindbrain, with moderate and low activities/staining in the midbrain and forebrain, respectively [86]. These results are consistent with high cPLA$_2$ levels/activities within myelin-rich regions. In fact, recent evidence has revealed a strong cPLA$_2$ immunoreactivity within axons and oligodendrocytes [67], further supporting our data/model. Notably, myelin-rich regions besides having a high abundance of phospholipids/sphingolipids, are also highly surrounded by astrocyte processes (where cPLA$_2$ expression has also been reported [135]). Taken together, AA release seems to occur preferentially within myelin-rich regions in a process involving oligodendrocyte, astrocyte, and/or axonal cPLA$_2$.

AD-related MAPK activation is independent of amyloid plaques

Our results revealed that all major MAPK pathways are activated by Aβ accumulation (both by APP$_{WT}$ overexpression and even further by accumulation of mutant Aβ) in the absence of fibrillary amyloid deposits. These results are in agreement with previous reports demonstrating that all major MAPK pathways (i.e., ERK, JNK, and p38 pathways) are activated in vulnerable neurons in patients with AD (reviewed in [137]). Activated MAPK signaling pathways have been proposed to significantly contribute to AD pathogenesis through various mechanisms including regulation of APP, β- and γ-secretases, and induction of neuronal apoptosis (reviewed in [57]). Here we are adding cPLA$_2$ (and potentially iPLA$_2$ as well) activation to the list of mechanisms by which MAPK mediates AD pathologies. Furthermore, we demonstrated for the first time that soluble oligomeric Aβ is sufficient to dramatically activate MAPK pathways in the absence of amyloid deposition and

that this Aβ-induced MAPK activation occurs in a PKC-independent manner.

The importance of wild-type APP controls for mutant APP transgenic studies

Our results revealed that over time overexpression of WT APP is sufficient to induce significant alterations in a broad set of lipid and proteins classes. Although some of these effects were further exacerbated in APP mutant Tg mice comparted to APP$_{WT}$ mice; we found several examples of markers that despite being altered between APP-Tg and non-Tg mice, were not significantly different between APP$_{WT}$ and APP mutant mice (like some PKC isoforms, GAPDH, and β-tubulin). Our results clearly demonstrate that unless APP$_{WT}$-Tg mice are included as controls, caution needs to be taken when concluding that a given effect is a consequence of a specific APP mutation(s) since such outcome could be partially or fully caused merely by transgenic APP gene expression.

Unfortunately, even though a plethora of mutant APP-Tg mouse models are currently available, only a handful of them have their respective APP$_{WT}$-Tg mouse control available. In fact, the vast majority of published AD animal studies have based their conclusions on comparisons between mutant APP-Tg mice versus non-Tg controls. We urge the AD field to consider incorporating APP$_{WT}$-Tg control mice into their experimental approaches whenever mutant APP-Tg mice are used. Alternatively, mutant APP-Tg results should be confirmed on human AD brain tissue and/or other non-Tg AD models, like the recently developed APP mutant knock-in mice [71]. Notably, our results also demonstrated that wild-type APP overexpression on its own is capable of modeling at least some aspects of AD (e.g., MAPK/cPLA$_2$ activation and free PUFA accumulation). Consistently, overexpression of wild-type hAPP causes early onset familial AD in human carriers with APP duplications [73, 92] and presumably in Down's syndrome [127].

Conclusions

1. Soluble oligomeric Aβ-induced PLA$_2$-mediated accumulation of free PUFAs leads to a disruption of lipid metabolism in AD independently of fibrillar amyloid.
2. cPLA$_2$ activity leads to the release and accumulation of free AA within myelin-rich regions, while iPLA$_2$ activity leads to the release and accumulation of free DHA within pyramidal neuron-rich regions.
3. Oligomeric Aβ is sufficient to dramatically activate MAPK pathways in the absence of amyloid plaques in a PKC-independent manner. This MAPK activation leads to increased PLA$_2$ phosphorylation/activity.

Palavicini *et al. Acta Neuropathologica Communications* (2017) 5:56

Page 14 of 17

Abbreviations

4-HNE: 4-hydroxynonenal; AA: Arachidonic acid; AD: Alzheimer's disease,; ADDL: Aβ derived diffusible ligand; apoE: apolipoprotein E; APP: Amyloid precursor protein; Aβ: Amyloid beta; CC: Corpus callosum; CIF: Calcium influx factor; COX: Cyclooxygenase; $cPLA_2$: group IV Ca^{2+}-dependent cytosolic; DHA: Docosahexaenoic acid; FA: Fatty acids; $iPLA_2$: group VI Ca^{2+}-independent PLA_2; LM: Lacunosum moleculare; MALDI: Matrix-assisted laser desorption/ ionization; MAPK: Mitogen-activated protein kinase; MDMS-SL: Multidimensional mass spectrometry-based shotgun lipidomics; MUFA: Monounsaturated fatty acid; NEFA: Nonesterified fatty acids; OA: oleic acid; Osk: Osaka; PKC: Protein kinase C; PLA_2: Phospholipase A_2; PUFA: Polyunsaturated fatty acid; Rad: Radiatum; $sPLA_2$: group II secretory PLA_2; Tg: Transgenic

Availability of data and materials

The datasets used and/or analyzed during the current study are available from the corresponding author on reasonable request.

Authors' contributions

JPP and XH conceived, designed, and coordinated the study. JPP wrote the manuscript, XH critically reviewed it. JPP and CW designed, performed, analyzed and prepared Figs. 1-2. LC provided technical assistance contributing to the preparation of multiple figures. JPP and KH designed, performed, analyzed, and prepared Figs. 3, 6, and 7. JPP designed, performed, analyzed, and prepared Fig. 5. JW designed, performed, analyzed, and prepared Fig. 4. HM and TT developed and maintained non-Tg, APP_WT, and APP_Osk mouse lines, they collected and provided the brain tissue used for the studies presented here. All authors reviewed and approved the final version of the manuscript.

Ethics approval

All applicable international, national, and/or institutional guidelines for the care and use of animals were followed.

Competing interest

The authors declare that they have no competing interests.

Publisher's Note

Springer Nature remains neutral with regard to jurisdictional claims in published maps and institutional affiliations.

Author details

[1]Center for Metabolic Origins of Disease, Sanford Burnham Prebys Medical Discovery Institute, 6400 Sanger Road, Orlando, FL 32827, USA. [2]Department of Translational Neuroscience, Osaka City University Graduate School of Medicine, 1-4-3 Asahimachi, Abeno-ku, Osaka 545-8585, Japan. [3]Department of Clinical Neuroscience, Osaka City University Graduate School of Medicine, 1-4-3 Asahimachi, Abeno-ku, Osaka 545-8585, Japan.

References

1. Adam-Klages S, Schwandner R, Luschen S, Ussat S, Kreder D, Kronke M (1998) Caspase-mediated inhibition of human cytosolic phospholipase A2 during apoptosis. J Immunol 161:5687–5694
2. Adams PB, Lawson S, Sanigorski A, Sinclair AJ (1996) Arachidonic acid to eicosapentaenoic acid ratio in blood correlates positively with clinical symptoms of depression. Lipids 31(Suppl):S157–S161
3. Almer G, Guegan C, Teismann P, Naini A, Rosoklija G, Hays AP, Chen C, Przedborski S (2001) Increased expression of the pro-inflammatory enzyme cyclooxygenase-2 in amyotrophic lateral sclerosis. Ann Neurol 49:176–185
4. Alzheimer A, Stelzmann RA, Schnitzlein HN, Murtagh FR (1995) An English translation of Alzheimer's 1907 paper, "Uber eine eigenartige Erkankung der Hirnrinde". Clin Anat 8:429–431. doi:10.1002/ca.980080612
5. Atsumi G, Murakami M, Kojima K, Hadano A, Tajima M, Kudo I (2000) Distinct roles of two intracellular phospholipase A2s in fatty acid release in the cell death pathway. Proteolytic fragment of type IVA cytosolic phospholipase A2alpha inhibits stimulus-induced arachidonate release, whereas that of type VI Ca2+–independent phospholipase A2 augments spontaneous fatty acid release. J Biol Chem 275:18248–18258. doi:10.1074/jbc.M000271200
6. Atsumi G, Tajima M, Hadano A, Nakatani Y, Murakami M, Kudo I (1998) Fas-induced arachidonic acid release is mediated by Ca2+–independent phospholipase A2 but not cytosolic phospholipase A2, which undergoes proteolytic inactivation. J Biol Chem 273:13870–13877
7. Barnett JM, McCollum GW, Penn JS (2010) Role of cytosolic phospholipase a(2) in retinal neovascularization. Invest Ophthalmol Vis Sci 51:1136–1142. doi:10.1167/iovs.09-3691
8. Bazan NG, Colangelo V, Lukiw WJ (2002) Prostaglandins and other lipid mediators in Alzheimer's disease. Prostaglandins Other Lipid Mediat 68-69: 197–210
9. Bonventre JV, Huang Z, Taheri MR, O'Leary E, Li E, Moskowitz MA, Sapirstein A (1997) Reduced fertility and postischaemic brain injury in mice deficient in cytosolic phospholipase A2. Nature 390:622–625. doi:10.1038/37635
10. Broniec A, Zadlo A, Pawlak A, Fuchs B, Klosinski R, Thompson D, Sarna T (2017) Interaction of plasmenylcholine with free radicals in selected model systems. Free Radic Biol Med 106:368–378. doi:10.1016/j.freeradbiomed.2017.02.029
11. Bucciantini M, Giannoni E, Chiti F, Baroni F, Formigli L, Zurdo J, Taddei N, Ramponi G, Dobson CM, Stefani M (2002) Inherent toxicity of aggregates implies a common mechanism for protein misfolding diseases. Nature 416: 507–511. doi:10.1038/416507a
12. Calon F, Lim GP, Yang F, Morihara T, Teter B, Ubeda O, Rostaing P, Triller A, Salem N Jr, Ashe KH, Frautschy SA, Cole GM (2004) Docosahexaenoic acid protects from dendritic pathology in an Alzheimer's disease mouse model. Neuron 43:633–645. doi:10.1016/j.neuron.2004.08.013
13. Castillo-Carranza DL, Guerrero-Munoz MJ, Sengupta U, Hernandez C, Barrett AD, Dineley K, Kayed R (2015) Tau immunotherapy modulates both pathological tau and upstream amyloid pathology in an Alzheimer's disease mouse model. J Neurosci 35:4857–4868. doi:10.1523/JNEUROSCI.4989-14.2015
14. Chalbot S, Zetterberg H, Blennow K, Fladby T, Grundke-Iqbal I, Iqbal K (2009) Cerebrospinal fluid secretory Ca2+–dependent phospholipase A2 activity is increased in Alzheimer disease. Clin Chem 55:2171–2179. doi:10.1373/clinchem.2009.130286
15. Chan RB, Oliveira TG, Cortes EP, Honig LS, Duff KE, Small SA, Wenk MR, Shui G, Di Paolo G (2012) Comparative lipidomic analysis of mouse and human brain with Alzheimer disease. J Biol Chem 287:2678–2688. doi:10.1074/jbc.M111.274142
16. Cheng H, Guan S, Han X (2006) Abundance of triacylglycerols in ganglia and their depletion in diabetic mice: implications for the role of altered triacylglycerols in diabetic neuropathy. J Neurochem 97:1288–1300. doi:10.1111/j.1471-4159.2006.03794.x
17. Cheng H, Jiang X, Han X (2007) Alterations in lipid homeostasis of mouse dorsal root ganglia induced by apolipoprotein E deficiency: a shotgun lipidomics study. J Neurochem 101:57–76. doi:10.1111/j.1471-4159.2006.04342.x
18. Cheng H, Wang M, Li JL, Cairns NJ, Han X (2013) Specific changes of sulfatide levels in individuals with pre-clinical Alzheimer's disease: an early event in disease pathogenesis. J Neurochem 127:733–738. doi:10.1111/jnc.12368
19. Cheng H, Xu J, McKeel DW Jr, Han X (2003) Specificity and potential mechanism of sulfatide deficiency in Alzheimer's disease: an electrospray ionization mass spectrometric study. Cell Mol Biol (Noisy-le-grand) 49:809–818
20. Clark JD, Lin LL, Kriz RW, Ramesha CS, Sultzman LA, Lin AY, Milona N, Knopf JL (1991) A novel arachidonic acid-selective cytosolic PLA2 contains a ca(2+)-dependent translocation domain with homology to PKC and GAP. Cell 65:1043–1051
21. Cleary JP, Walsh DM, Hofmeister JJ, Shankar GM, Kuskowski MA, Selkoe DJ, Ashe KH (2005) Natural oligomers of the amyloid-beta protein specifically disrupt cognitive function. Nat Neurosci 8:79–84. doi:10.1038/nn1372
22. Colangelo V, Schurr J, Ball MJ, Pelaez RP, Bazan NG, Lukiw WJ (2002) Gene expression profiling of 12633 genes in Alzheimer hippocampal CA1: transcription and neurotrophic factor down-regulation and up-regulation of apoptotic and pro-inflammatory signaling. J Neurosci Res 70:462–473. doi:10.1002/jnr.10351
23. Couttas TA, Kain N, Suchowerska AK, Quek LE, Turner N, Fath T, Garner B, Don AS (2016) Loss of ceramide synthase 2 activity, necessary for myelin

Palavicini *et al. Acta Neuropathologica Communications* (2017) 5:56

Page 15 of 17

biosynthesis, precedes tau pathology in the cortical pathogenesis of Alzheimer's disease. Neurobiol Aging 43:89–100. doi:10.1016/j.neurobiolaging.2016.03.027

24. Cummings BS, McHowat J, Schnellmann RG (2000) Phospholipase a(2)s in cell injury and death. J Pharmacol Exp Ther 294:793–799

25. Cunnane SC, Schneider JA, Tangney C, Tremblay-Mercier J, Fortier M, Bennett DA, Morris MC (2012) Plasma and brain fatty acid profiles in mild cognitive impairment and Alzheimer's disease. J Alzheimers Dis 29:691–697. doi:10.3233/JAD-2012-110629

26. Cutler RG, Kelly J, Storie K, Pedersen WA, Tammara A, Hatanpaa K, Troncoso JC, Mattson MP (2004) Involvement of oxidative stress-induced abnormalities in ceramide and cholesterol metabolism in brain aging and Alzheimer's disease. Proc Natl Acad Sci U S A 101:2070–2075. doi:10.1073/pnas.0305799101

27. De Felice FG, Velasco PT, Lambert MP, Viola K, Fernandez SJ, Ferreira ST, Klein WL (2007) Abeta oligomers induce neuronal oxidative stress through an N-methyl-D-aspartate receptor-dependent mechanism that is blocked by the Alzheimer drug memantine. J Biol Chem 282:11590–11601. doi:10.1074/jbc.M607483200

28. Diez E, Chilton FH, Stroup G, Mayer RJ, Winkler JD, Fonteh AN (1994) Fatty acid and phospholipid selectivity of different phospholipase A2 enzymes studied by using a mammalian membrane as substrate. Biochem J 301(Pt 3):721–726

29. Dodart JC, Bales KR, Gannon KS, Greene SJ, DeMattos RB, Mathis C, DeLong CA, Wu S, Wu X, Holtzman DM, Paul SM (2002) Immunization reverses memory deficits without reducing brain Abeta burden in Alzheimer's disease model. Nat Neurosci 5:452–457. doi:10.1038/nn842

30. El Mahdani NE, Ameyar M, Cai Z, Colard O, Masliah J, Chouaib S (2000) Resistance to TNF-induced cytotoxicity correlates with an abnormal cleavage of cytosolic phospholipase A2. J Immunol 165:6756–6761

31. Fang KM, Chang WL, Wang SM, Su MJ, Wu ML (2008) Arachidonic acid induces both Na+ and Ca2+ entry resulting in apoptosis. J Neurochem 104:1177–1189. doi:10.1111/j.1471-4159.2007.05022.x

32. Farooqui AA, Horrocks LA (2004) Brain phospholipases A2: a perspective on the history. Prostaglandins Leukot Essent Fatty Acids 71:161–169. doi:10.1016/j.plefa.2004.03.004

33. Fuchs B, Schiller J (2009) Lysophospholipids: their generation, physiological role and detection. Are they important disease markers? Mini Rev Med Chem 9:368–378

34. Geijsen N, Dijkers PF, Lammers JJ, Koenderman L, Coffer PJ (2000) Cytokine-mediated cPLA(2) phosphorylation is regulated by multiple MAPK family members. FEBS Lett 471:83–88

35. Ghosh M, Tucker DE, Burchett SA, Leslie CC (2006) Properties of the group IV phospholipase A2 family. Prog Lipid Res 45:487–510. doi:10.1016/j.plipres.2006.05.003

36. Gong Y, Chang L, Viola KL, Lacor PN, Lambert MP, Finch CE, Krafft GA, Klein WL (2003) Alzheimer's disease-affected brain: presence of oligomeric a beta ligands (ADDLs) suggests a molecular basis for reversible memory loss. Proc Natl Acad Sci U S A 100:10417–10422. doi:10.1073/pnas.1834302100

37. Green JT, Orr SK, Bazinet RP (2008) The emerging role of group VI calcium-independent phospholipase A2 in releasing docosahexaenoic acid from brain phospholipids. J Lipid Res 49:939–944. doi:10.1194/jlr.R700017-JLR200

38. Green KN, Martinez-Coria H, Khashwji H, Hall EB, Yurko-Mauro KA, Ellis L, LaFerla FM (2007) Dietary docosahexaenoic acid and docosapentaenoic acid ameliorate amyloid-beta and tau pathology via a mechanism involving presenilin 1 levels. J Neurosci 27:4385–4395. doi:10.1523/JNEUROSCI.0055-07.2007

39. Gregory A, Westaway SK, Holm IE, Kotzbauer PT, Hogarth P, Sonek S, Coryell JC, Nguyen TM, Nardocci N, Zorzi G, Rodriguez D, Desguerre I, Bertini E, Simonati A, Levinson B, Dias C, Barbot C, Carrilho I, Santos M, Malik I, Gitschier J, Hayflick SJ (2008) Neurodegeneration associated with genetic defects in phospholipase a(2). Neurology 71:1402–1409. doi:10.1212/01.wnl.0000327094.67726.28

40. Guo YL, Kang B, Yang LJ, Williamson JR (1999) Tumor necrosis factor-alpha and ceramide induce cell death through different mechanisms in rat mesangial cells. Am J Phys 276:F390–F397

41. Han X (2007) Potential mechanisms contributing to sulfatide depletion at the earliest clinically recognizable stage of Alzheimer's disease: a tale of shotgun lipidomics. J Neurochem 103(Suppl 1):171–179. doi:10.1111/j.1471-4159.2007.04708.x

42. Han X (2016) Lipidomics for studying metabolism. Nat Rev Endocrinol 12:668–679. doi:10.1038/nrendo.2016.98

43. Han X, MH D, DW MK Jr, Kelley J, Morris JC (2002) Substantial sulfatide deficiency and ceramide elevation in very early Alzheimer's disease: potential role in disease pathogenesis. J Neurochem 82:809–818

44. Han X, Fagan AM, Cheng H, Morris JC, Xiong C, Holtzman DM (2003) Cerebrospinal fluid sulfatide is decreased in subjects with incipient dementia. Ann Neurol 54:115–119. doi:10.1002/ana.10618

45. Han X, Gross RW (2005) Shotgun lipidomics: multidimensional MS analysis of cellular lipidomes. Expert review of proteomics 2:253–264. doi:10.1586/14789450.2.2.253

46. Han X, Holtzman DM, McKeel DW Jr (2001) Plasmalogen deficiency in early Alzheimer's disease subjects and in animal models: molecular characterization using electrospray ionization mass spectrometry. J Neurochem 77:1168–1180

47. Han X, Yang K, Gross RW (2008) Microfluidics-based electrospray ionization enhances the intrasource separation of lipid classes and extends identification of individual molecular species through multi-dimensional mass spectrometry: development of an automated high-throughput platform for shotgun lipidomics. Rapid communications in mass spectrometry : RCM 22:2115–2124. doi:10.1002/rcm.3595

48. Hardy J, Selkoe DJ (2002) The amyloid hypothesis of Alzheimer's disease: progress and problems on the road to therapeutics. Science 297:353–356. doi:10.1126/science.1072994

49. Hardy JA, Higgins GA (1992) Alzheimer's disease: the amyloid cascade hypothesis. Science 256:184–185

50. Hefner Y, Borsch-Haubold AG, Murakami M, Wilde JI, Pasquet S, Schieltz D, Ghomashchi F, Yates JR 3rd, Armstrong CG, Paterson A, Cohen P, Fukunaga R, Hunter T, Kudo I, Watson SP, Gelb MH (2000) Serine 727 phosphorylation and activation of cytosolic phospholipase A2 by MNK1-related protein kinases. J Biol Chem 275:37542–37551. doi:10.1074/jbc.M003395200

51. Hu C, Wang M, Han X (2017) Shotgun lipidomics in substantiating lipid peroxidation in redox biology: methods and applications. Redox Biol 12:946–955. doi:10.1016/j.redox.2017.04.030

52. Joachim CL, Selkoe DJ (1992) The seminal role of beta-amyloid in the pathogenesis of Alzheimer disease. Alzheimer Dis Assoc Disord 6:7–34

53. Kayed R, Head E, Thompson JL, McIntire TM, Milton SC, Cotman CW, Glabe CG (2003) Common structure of soluble amyloid oligomers implies common mechanism of pathogenesis. Science 300:486–489. doi:10.1126/science.1079469

54. Kennedy BP, Payette P, Mudgett J, Vadas P, Pruzanski W, Kwan M, Tang C, Rancourt DE, Cromlish WA (1995) A natural disruption of the secretory group II phospholipase A2 gene in inbred mouse strains. J Biol Chem 270:22378–22385

55. Keranen LM, Dutil EM, Newton AC (1995) Protein kinase C is regulated in vivo by three functionally distinct phosphorylations. Curr Biol 5:1394–1403

56. Khateeb S, Flusser H, Ofir R, Shelef I, Narkis G, Vardi G, Shorer Z, Levy R, Galil A, Elbedour K, Birk OS (2006) PLA2G6 mutation underlies infantile neuroaxonal dystrophy. Am J Hum Genet 79:942–948. doi:10.1086/508572

57. Kim EK, Choi EJ (2010) Pathological roles of MAPK signaling pathways in human diseases. Biochim Biophys Acta 1802:396–405. doi:10.1016/j.bbadis.2009.12.009

58. Koffie RM, Hyman BT, Spires-Jones TL (2011) Alzheimer's disease: synapses gone cold. Mol Neurodegener 6:63. doi:10.1186/1750-1326-6-63

59. Kramer RM, Roberts EF, Manetta J, Putnam JE (1991) The Ca2(+)-sensitive cytosolic phospholipase A2 is a 100-kDa protein in human monoblast U937 cells. J Biol Chem 266:5268–5272

60. Kramer RM, Roberts EF, Um SL, Borsch-Haubold AG, Watson SP, Fisher MJ, Jakubowski JA (1996) p38 mitogen-activated protein kinase phosphorylates cytosolic phospholipase A2 (cPLA2) in thrombin-stimulated platelets. Evidence that proline-directed phosphorylation is not required for mobilization of arachidonic acid by cPLA2. J Biol Chem 271:27723–27729

61. Kudo I, Murakami M (2002) Phospholipase A2 enzymes. Prostaglandins Other Lipid Mediat 68-69:3–58

62. Lacor PN, Buniel MC, Furlow PW, Clemente AS, Velasco PT, Wood M, Viola KL, Klein WL (2007) Abeta oligomer-induced aberrations in synapse composition, shape, and density provide a molecular basis for loss of connectivity in Alzheimer's disease. The Journal of neuroscience : the official journal of the Society for Neuroscience 27:796–807. doi:10.1523/JNEUROSCI.3501-06.2007

63. Lambert MP, Barlow AK, Chromy BA, Edwards C, Freed R, Liosatos M, Morgan TE, Rozovsky I, Trommer B, Viola KL, Wals P, Zhang C, Finch CE, Krafft GA, Klein WL (1998) Diffusible, nonfibrillar ligands derived from Abeta1-42 are potent central nervous system neurotoxins. Proc Natl Acad Sci U S A 95:6448–6453

64. Lesne S, Koh MT, Kotilinek L, Kayed R, Glabe CG, Yang A, Gallagher M, Ashe KH (2006) A specific amyloid-beta protein assembly in the brain impairs memory. Nature 440:352–357. doi:10.1038/nature04533

Palavicini *et al. Acta Neuropathologica Communications* (2017) 5:56

Page 16 of 17

65. Lim GP, Calon F, Morihara T, Yang F, Teter B, Ubeda O, Salem N Jr, Frautschy SA, Cole GM (2005) A diet enriched with the omega-3 fatty acid docosahexaenoic acid reduces amyloid burden in an aged Alzheimer mouse model. J Neurosci 25: 3032–3040. doi:10.1523/JNEUROSCI.4225-04.2005

66. Lin LL, Wartmann M, Lin AY, Knopf JL, Seth A, Davis RJ (1993) cPLA2 is phosphorylated and activated by MAP kinase. Cell 72:269–278

67. Liu NK, Deng LX, Zhang YP, Lu QB, Wang XF, Hu JG, Oakes E, Bonventre JV, Shields CB, Xu XM (2014) Cytosolic phospholipase A2 protein as a novel therapeutic target for spinal cord injury. Ann Neurol 75:644–658. doi:10.1002/ana.24134

68. Lue LF, Kuo YM, Roher AE, Brachova L, Shen Y, Sue L, Beach T, Kurth JH, Rydel RE, Rogers J (1999) Soluble amyloid beta peptide concentration as a predictor of synaptic change in Alzheimer's disease. Am J Pathol 155:853–862

69. Lukiw WJ, Cui JG, Marcheselli VL, Bodker M, Botkjaer A, Gotlinger K, Serhan CN, Bazan NG (2005) A role for docosahexaenoic acid-derived neuroprotectin D1 in neural cell survival and Alzheimer disease. J Clin Invest 115:2774–2783. doi:10.1172/JCI25420

70. Malik I, Turk J, Mancuso DJ, Montier L, Wohltmann M, Wozniak DF, Schmidt RE, Gross RW, Kotzbauer PT (2008) Disrupted membrane homeostasis and accumulation of ubiquitinated proteins in a mouse model of infantile neuroaxonal dystrophy caused by PLA2G6 mutations. Am J Pathol 172:406–416. doi:10.2353/ajpath.2008.070823

71. Masuda A, Kobayashi Y, Kogo N, Saito T, Saido TC, Itohara S (2016) Cognitive deficits in single app knock-in mouse models. Neurobiol Learn Mem 135: 73–82. doi:10.1016/j.nlm.2016.07.001

72. McLean CA, Cherny RA, Fraser FW, Fuller SJ, Smith MJ, Beyreuther K, Bush AI, Masters CL (1999) Soluble pool of Abeta amyloid as a determinant of severity of neurodegeneration in Alzheimer's disease. Ann Neurol 46:860–866

73. McNaughton D, Knight W, Guerreiro R, Ryan N, Lowe J, Poulter M, Nicholl DJ, Hardy J, Revesz T, Lowe J, Rossor M, Collinge J, Mead S (2012) Duplication of amyloid precursor protein (APP), but not prion protein (PRNP) gene is a significant cause of early onset dementia in a large UK series. Neurobiol Aging 33(426):e413–e421. doi:10.1016/j.neurobiolaging.2010.10.010

74. Menard C, Patenaude C, Massicotte G (2005) Phosphorylation of AMPA receptor subunits is differentially regulated by phospholipase A2 inhibitors. Neurosci Lett 389:51–56. doi:10.1016/j.neulet.2005.07.012

75. Meyer MC, Kell PJ, Creer MH, McHowat J (2005) Calcium-independent phospholipase A2 is regulated by a novel protein kinase C in human coronary artery endothelial cells. Am J Physiol Cell Physiol 288:C475–C482. doi:10.1152/ajpcell.00306.2004

76. Moore SA (1994) Local synthesis and targeting of essential fatty acids at the cellular interface between blood and brain: a role for cerebral endothelium and astrocytes in the accretion of CNS docosahexaenoic acid. World Rev Nutr Diet 75:128–133

77. Moore SA (2001) Polyunsaturated fatty acid synthesis and release by brain-derived cells in vitro. J Mol Neurosci 16:195–200; discussion 215-121. doi:10.1385/JMN:16:2-3:195

78. Morgan NV, Westaway SK, Morton JE, Gregory A, Gissen P, Sonek S, Cangul H, Coryell J, Canham N, Nardocci N, Zorzi G, Pasha S, Rodriguez D, Desguerre I, Mubaidin A, Bertini E, Trembath RC, Simonati A, Schanen C, Johnson CA, Levinson B, Woods CG, Wilmot B, Kramer P, Gitschier J, Maher ER, Hayflick SJ (2006) PLA2G6, encoding a phospholipase A2, is mutated in neurodegenerative disorders with high brain iron. Nat Genet 38:752–754. doi:10.1038/ng1826

79. Morris MC, Evans DA, Bienias JL, Tangney CC, Bennett DA, Wilson RS, Aggarwal N, Schneider J (2003) Consumption of fish and n-3 fatty acids and risk of incident Alzheimer disease. Arch Neurol 60:940–946. doi:10.1001/archneur.60.7.940

80. Moses GS, Jensen MD, Lue LF, Walker DG, Sun AY, Simonyi A, Sun GY (2006) Secretory PLA2-IIA: a new inflammatory factor for Alzheimer's disease. J Neuroinflammation 3:28. doi:10.1186/1742-2094-3-28

81. Murakami M, Nakatani Y, Atsumi G, Inoue K, Kudo I (1997) Regulatory functions of phospholipase A2. Crit Rev Immunol 17:225–283

82. Nasaruddin ML, Holscher C, Kehoe P, Graham SF, Green BD (2016) Wide-ranging alterations in the brain fatty acid complement of subjects with late Alzheimer's disease as detected by GC-MS. Am J Transl Res 8: 154–165

83. Nishitsuji K, Tomiyama T, Ishibashi K, Ito K, Teraoka R, Lambert MP, Klein WL, Mori H (2009) The E693Delta mutation in amyloid precursor protein increases intracellular accumulation of amyloid beta oligomers and causes endoplasmic reticulum stress-induced apoptosis in cultured cells. Am J Pathol 174:957–969. doi:10.2353/ajpath.2009.080480

84. Nomura S, Umeda T, Tomiyama T, Mori H (2013) The E693Delta (Osaka) mutation in amyloid precursor protein potentiates cholesterol-mediated intracellular amyloid beta toxicity via its impaired cholesterol efflux. J Neurosci Res 91:1541–1550. doi:10.1002/jnr.23278

85. Oda T, Wals P, Osterburg HH, Johnson SA, Pasinetti GM, Morgan TE, Rozovsky I, Stine WB, Snyder SW, Holzman TF et al (1995) Clusterin (apoJ) alters the aggregation of amyloid beta-peptide (a beta 1-42) and forms slowly sedimenting a beta complexes that cause oxidative stress. Exp Neurol 136:22–31

86. Ong WY, Sandhya TL, Horrocks LA, Farooqui AA (1999) Distribution of cytoplasmic phospholipase A2 in the normal rat brain. J Hirnforsch 39:391–400

87. Ong WY, Yeo JF, Ling SF, Farooqui AA (2005) Distribution of calcium-independent phospholipase A2 (iPLA 2) in monkey brain. J Neurocytol 34: 447–458. doi:10.1007/s11068-006-8730-4

88. Phillis JW, Horrocks LA, Farooqui AA (2006) Cyclooxygenases, lipoxygenases, and epoxygenases in CNS: their role and involvement in neurological disorders. Brain Res Rev 52:201–243. doi:10.1016/j.brainresrev.2006.02.002

89. Pratico D, Uryu K, Leight S, Trojanoswki JQ, Lee VM (2001) Increased lipid peroxidation precedes amyloid plaque formation in an animal model of Alzheimer amyloidosis. J Neurosci 21:4183–4187

90. Rao JS, Lee HJ, Rapoport SI, Bazinet RP (2008) Mode of action of mood stabilizers: is the arachidonic acid cascade a common target? Mol Psychiatry 13:585–596. doi:10.1038/mp.2008.31

91. Rodriguez JJ, Olabarria M, Chvatal A, Verkhratsky A (2009) Astroglia in dementia and Alzheimer's disease. Cell Death Differ 16:378–385. doi:10.1038/cdd.2008.172

92. Rovelet-Lecrux A, Hannequin D, Raux G, Le Meur N, Laquerriere A, Vital A, Dumanchin C, Feuillette S, Brice A, Vercelletto M, Dubas F, Frebourg T, Campion D (2006) APP locus duplication causes autosomal dominant early-onset Alzheimer disease with cerebral amyloid angiopathy. Nat Genet 38: 24–26. doi:10.1038/ng1718

93. Ruiperez V, Casas J, Balboa MA, Balsinde J (2007) Group V phospholipase A2-derived lysophosphatidylcholine mediates cyclooxygenase-2 induction in lipopolysaccharide-stimulated macrophages. J Immunol 179:631–638

94. Sanchez-Mejia RO, Mucke L (2010) Phospholipase A2 and arachidonic acid in Alzheimer's disease. Biochim Biophys Acta 1801:784–790. doi:10.1016/j.bbalip.2010.05.013

95. Sanchez-Mejia RO, Newman JW, Toh S, Yu GQ, Zhou Y, Halabisky B, Cisse M, Scearce-Levie K, Cheng IH, Gan L, Palop JJ, Bonventre JV, Mucke L (2008) Phospholipase A2 reduction ameliorates cognitive deficits in a mouse model of Alzheimer's disease. Nat Neurosci 11:1311–1318. doi:10.1038/nn.2213

96. Sato H, Kato R, Isogai Y, Saka G, Ohtsuki M, Taketomi Y, Yamamoto K, Tsutsumi K, Yamada J, Masuda S, Ishikawa Y, Ishii T, Kobayashi T, Ikeda K, Taguchi R, Hatakeyama S, Hara S, Kudo I, Itabe H, Murakami M (2008) Analyses of group III secreted phospholipase A2 transgenic mice reveal potential participation of this enzyme in plasma lipoprotein modification, macrophage foam cell formation, and atherosclerosis. J Biol Chem 283: 33483–33497. doi:10.1074/jbc.M804628200

97. Selkoe DJ (1991) Alzheimer's disease. In the beginning Nature 354:432–433. doi:10.1038/354432a0

98. Selkoe DJ (2002) Alzheimer's disease is a synaptic failure. Science 298:789–791. doi:10.1126/science.1074069

99. Serhan CN, Arita M, Hong S, Gotlinger K (2004) Resolvins, docosatrienes, and neuroprotectins, novel omega-3-derived mediators, and their endogenous aspirin-triggered epimers. Lipids 39:1125–1132

100. Shelat PB, Chalimoniuk M, Wang JH, Strosznajder JB, Lee JC, Sun AY, Simonyi A, Sun GY (2008) Amyloid beta peptide and NMDA induce ROS from NADPH oxidase and AA release from cytosolic phospholipase A2 in cortical neurons. J Neurochem 106:45–55. doi:10.1111/j.1471-4159.2008.05347.x

101. Shikano M, Masuzawa Y, Yazawa K, Takayama K, Kudo I, Inoue K (1994) Complete discrimination of docosahexaenoate from arachidonate by 85 kDa cytosolic phospholipase A2 during the hydrolysis of diacyl- and alkenylacylglycerophosphoethanolamine. Biochim Biophys Acta 1212:211–216

102. Shinzawa K, Sumi H, Ikawa M, Matsuoka Y, Okabe M, Sakoda S, Tsujimoto Y (2008) Neuroaxonal dystrophy caused by group VIA phospholipase A2 deficiency in mice: a model of human neurodegenerative disease. J Neurosci 28:2212–2220. doi:10.1523/JNEUROSCI.4354-07.2008

103. Singh M (2005) Essential fatty acids, DHA and human brain. Indian J Pediatr 72:239–242

104. Smani T, Zakharov SI, Csutora P, Leno E, Trepakova ES, Bolotina VM (2004) A novel mechanism for the store-operated calcium influx pathway. Nat Cell Biol 6:113–120. doi:10.1038/ncb1089

Palavicini *et al. Acta Neuropathologica Communications* (2017) 5:56

Page 17 of 17

105. Snowden SG, Ebshiana AA, Hye A, An Y, Pletnikova O, O'Brien R, Troncoso J, Legido-Quigley C, Thambisetty M (2017) Association between fatty acid metabolism in the brain and Alzheimer disease neuropathology and cognitive performance: a nontargeted metabolomic study. PLoS Med 14: e1002266. doi:10.1371/journal.pmed.1002266

106. Spector AA, Norris AW (2007) Action of epoxyeicosatrienoic acids on cellular function. Am J Physiol Cell Physiol 292:C996–1012. doi:10.1152/ajpcell.00402.2006

107. Standridge JB (2006) Vicious cycles within the neuropathophysiologic mechanisms of Alzheimer's disease. Curr Alzheimer Res 3:95–108

108. Stephenson D, Rash K, Smalstig B, Roberts E, Johnstone E, Sharp J, Panetta J, Little S, Kramer R, Clemens J (1999) Cytosolic phospholipase A2 is induced in reactive glia following different forms of neurodegeneration. Glia 27:110–128

109. Stephenson DT, Lemere CA, Selkoe DJ, Clemens JA (1996) Cytosolic phospholipase A2 (cPLA2) immunoreactivity is elevated in Alzheimer's disease brain. Neurobiol Dis 3:51–63. doi:10.1006/nbdi.1996.0005

110. Sun GY, Horrocks LA (1970) The acyl and alk-1-enyl groups of the major phosphoglycerides from ox brain myelin and mouse brain microsomal, mitochondrial and myelin fractions. Lipids 5:1006–1012

111. Sun GY, Xu J, Jensen MD, Simonyi A (2004) Phospholipase A2 in the central nervous system: implications for neurodegenerative diseases. J Lipid Res 45: 205–213. doi:10.1194/jlr.R300016-JLR200

112. Takuma H, Teraoka R, Mori H, Tomiyama T (2008) Amyloid-beta E22Delta variant induces synaptic alteration in mouse hippocampal slices. Neuroreport 19:615–619. doi:10.1097/WNR.0b013e3282fb78c4

113. Talib LL, Hototian SR, Joaquim HP, Forlenza OV, Gattaz WF (2015) Increased iPLA2 activity and levels of phosphorylated GSK3B in platelets are associated with donepezil treatment in Alzheimer's disease patients. Eur Arch Psychiatry Clin Neurosci 265:701–706. doi:10.1007/s00406-015-0600-6

114. Teismann P, Vila M, Choi DK, Tieu K, Wu DC, Jackson-Lewis V, Przedborski S (2003) COX-2 and neurodegeneration in Parkinson's disease. Ann N Y Acad Sci 991:272–277

115. Tomiyama T, Matsuyama S, Iso H, Umeda T, Takuma H, Ohnishi K, Ishibashi K, Teraoka R, Sakama N, Yamashita T, Nishitsuji K, Ito K, Shimada H, Lambert MP, Klein WL, Mori H (2010) A mouse model of amyloid beta oligomers: their contribution to synaptic alteration, abnormal tau phosphorylation, glial activation, and neuronal loss in vivo. J Neurosci 30:4845–4856. doi:10.1523/JNEUROSCI.5825-09.2010

116. Tomiyama T, Nagata T, Shimada H, Teraoka R, Fukushima A, Kanemitsu H, Takuma H, Kuwano R, Imagawa M, Ataka S, Wada Y, Yoshioka E, Nishizaki T, Watanabe Y, Mori H (2008) A new amyloid beta variant favoring oligomerization in Alzheimer's-type dementia. Ann Neurol 63:377–387. doi:10.1002/ana.21321

117. Tucker DE, Gijon MA, Spencer DM, Qiu ZH, Gelb MH, Leslie CC (2008) Regulation of cytosolic phospholipase A2alpha by hsp90 and a p54 kinase in okadaic acid-stimulated macrophages. J Leukoc Biol 84:798–806. doi:10.1189/jlb.0308197

118. Umeda T, Ono K, Sakai A, Yamashita M, Mizuguchi M, Klein WL, Yamada M, Mori H, Tomiyama T (2016) Rifampicin is a candidate preventive medicine against amyloid-beta and tau oligomers. Brain 139:1568–1586. doi:10.1093/brain/aww042

119. Voelkel-Johnson C, Entingh AJ, Wold WS, Gooding LR, Laster SM (1995) Activation of intracellular proteases is an early event in TNF-induced apoptosis. J Immunol 154:1707–1716

120. Walsh DM, Klyubin I, Fadeeva JV, Cullen WK, Anwyl R, Wolfe MS, Rowan MJ, Selkoe DJ (2002) Naturally secreted oligomers of amyloid beta protein potently inhibit hippocampal long-term potentiation in vivo. Nature 416: 535–539. doi:10.1038/416535a

121. Wang DC, Sun CH, Liu LY, Sun XH, Jin XW, Song WL, Liu XQ, Wan XL (2012) Serum fatty acid profiles using GC-MS and multivariate statistical analysis: potential biomarkers of Alzheimer's disease. Neurobiol Aging 33:1057–1066. doi:10.1016/j.neurobiolaging.2010.09.013

122. Wang HW, Pasternak JF, Kuo H, Ristic H, Lambert MP, Chromy B, Viola KL, Klein WL, Stine WB, Krafft GA, Trommer BL (2002) Soluble oligomers of beta amyloid (1-42) inhibit long-term potentiation but not long-term depression in rat dentate gyrus. Brain Res 924:133–140

123. Wang J, Dickson DW, Trojanowski JQ, Lee VM (1999) The levels of soluble versus insoluble brain Abeta distinguish Alzheimer's disease from normal and pathologic aging. Exp Neurol 158:328–337. doi:10.1006/exnr.1999.7085

124. Wang J, Qiu S, Chen S, Xiong C, Liu H, Wang J, Zhang N, Hou J, He Q, Nie Z (2015) MALDI-TOF MS imaging of metabolites with a N-(1-naphthyl) ethylenediamine dihydrochloride matrix and its application to colorectal cancer liver metastasis. Anal Chem 87:422–430. doi:10.1021/ac504294s

125. Wang M, Wang C, Han X (2016) Selection of internal standards for accurate quantification of complex lipid species in biological extracts by electrospray ionization mass spectrometry-what, how and why? Mass Spectrom Rev. doi:10.1002/mas.21492

126. Wang Q, Tang XN, Yenari MA (2007) The inflammatory response in stroke. J Neuroimmunol 184:53–68. doi:10.1016/j.jneuroim.2006.11.014

127. Wiseman FK, Al-Janabi T, Hardy J, Karmiloff-Smith A, Nizetic D, Tybulewicz VL, Fisher EM, Strydom A (2015) A genetic cause of Alzheimer disease: mechanistic insights from down syndrome. Nat Rev Neurosci 16:564–574. doi:10.1038/nrn3983

128. Wissing D, Mouritzen H, Egeblad M, Poirier GG, Jaattela M (1997) Involvement of caspase-dependent activation of cytosolic phospholipase A2 in tumor necrosis factor-induced apoptosis. Proc Natl Acad Sci U S A 94:5073–5077

129. Wolf MJ, Gross RW (1996) The calcium-dependent association and functional coupling of calmodulin with myocardial phospholipase A2. Implications for cardiac cycle-dependent alterations in phospholipolysis J Biol Chem 271:20989–20992

130. Wolf MJ, Wang J, Turk J, Gross RW (1997) Depletion of intracellular calcium stores activates smooth muscle cell calcium-independent phospholipase A2. A novel mechanism underlying arachidonic acid mobilization J Biol Chem 272:1522–1526

131. Xu J, Weng YI, Simonyi A, Krugh BW, Liao Z, Weisman GA, Sun GY (2002) Role of PKC and MAPK in cytosolic PLA2 phosphorylation and arachadonic acid release in primary murine astrocytes. J Neurochem 83:259–270

132. Yang HC, Mosior M, Johnson CA, Chen Y, Dennis EA (1999) Group-specific assays that distinguish between the four major types of mammalian phospholipase A2. Anal Biochem 269:278–288. doi:10.1006/abio.1999.4053

133. Yang K, Cheng H, Gross RW, Han X (2009) Automated lipid identification and quantification by multidimensional mass spectrometry-based shotgun lipidomics. Anal Chem 81:4356–4368. doi:10.1021/ac900241u

134. Zalewski A, Macphee C (2005) Role of lipoprotein-associated phospholipase A2 in atherosclerosis: biology, epidemiology, and possible therapeutic target. Arterioscler Thromb Vasc Biol 25:923–931. doi:10.1161/01.ATV.0000160551.21962.a7

135. Zanassi P, Paolillo M, Schinelli S (1998) Coexpression of phospholipase A2 isoforms in rat striatal astrocytes. Neurosci Lett 247:83–86

136. Zhao X, Wang D, Zhao Z, Xiao Y, Sengupta S, Xiao Y, Zhang R, Lauber K, Wesselborg S, Feng L, Rose TM, Shen Y, Zhang J, Prestwich G, Xu Y (2006) Caspase-3-dependent activation of calcium-independent phospholipase A2 enhances cell migration in non-apoptotic ovarian cancer cells. J Biol Chem 281:29357–29368. doi:10.1074/jbc.M513105200

137. Zhu X, Lee HG, Raina AK, Perry G, Smith MA (2002) The role of mitogen-activated protein kinase pathways in Alzheimer's disease. Neurosignals 11: 270-281. Doi:67426